



Contents lists available at ScienceDirect

European Journal of Medicinal Chemistry

journal homepage: <http://www.elsevier.com/locate/ejmech>

A greener protocol for the synthesis of phosphorochalcogenoates: Antioxidant and free radical scavenging activities



Daniela H. Mailahn^a, Lucas E.B. Iarocz^a, Patrick C. Nobre^a, Gelson Perin^a, Airton Sinott^b, Ana Paula Pesarico^b, Paloma T. Birmann^b, Lucielli Savegnago^b, Márcio S. Silva^{a,*}

^a LASOL - CCQFA, Universidade Federal de Pelotas - UFPel, P.O. Box 354, 96010-900, Pelotas, RS, Brazil

^b Programa de Pós-Graduação Em Biotecnologia, Grupo de Pesquisa Em Neurobiotecnologia, Centro de Biotecnologia, Universidade Federal de Pelotas, RS, Brazil

ARTICLE INFO

Article history:

Received 3 September 2020

Received in revised form

17 November 2020

Accepted 22 November 2020

Available online 27 November 2020

ABSTRACT

In this contribution, a metal- and base-free protocol has been developed for the synthesis of phosphorochalcogenoates (Se and Te) by using DMSO as solvent at 50 °C. A variety of phosphorochalcogenoates were prepared from diorganyl dichalcogenides and *H*-phosphonates, leading to the formation of a Chal-P(O) bond, in a rapid procedure with good to excellent yields. A full structural elucidation of products was accessed by 1D and 2D NMR, IR, CGMS, and HRMS analyses, and a stability evaluation of the phosphorochalcogenoates was performed for an effective operational description of this simple and feasible method. Typical ⁷⁷Se{¹H} ($\delta_{\text{Se}} = 866.0$ ppm), ¹²⁵Te{¹H} ($\delta_{\text{Te}} = 422.0$ ppm) and ³¹P{¹H} ($\delta_{\text{P}} = -1.0, -13.0$ and -15.0 ppm) NMR chemical shifts were imperative to confirm the byproducts, in which this stability study was also important to select some products for pharmacological screening. The phosphorochalcogenoates were screened *in vitro* and *ex vivo* tests for the antioxidant potential and free radical scavenging activity, as well as to investigate toxicity in mice through of the plasma levels of markers of renal and hepatic damage. The pharmacological screening of phosphorochalcogenoates indicated that compounds have antioxidant propriety in different assays and not changes plasma levels of markers of renal and hepatic damage, with excision of **3g** compound that increased plasma creatinine levels and decreased plasma urea levels when compared to control group in the blood mice. Thus, these compounds can be promising synthetic antioxidants that provide protection against oxidative diseases.

© 2020 Elsevier Masson SAS. All rights reserved.

1. Introduction

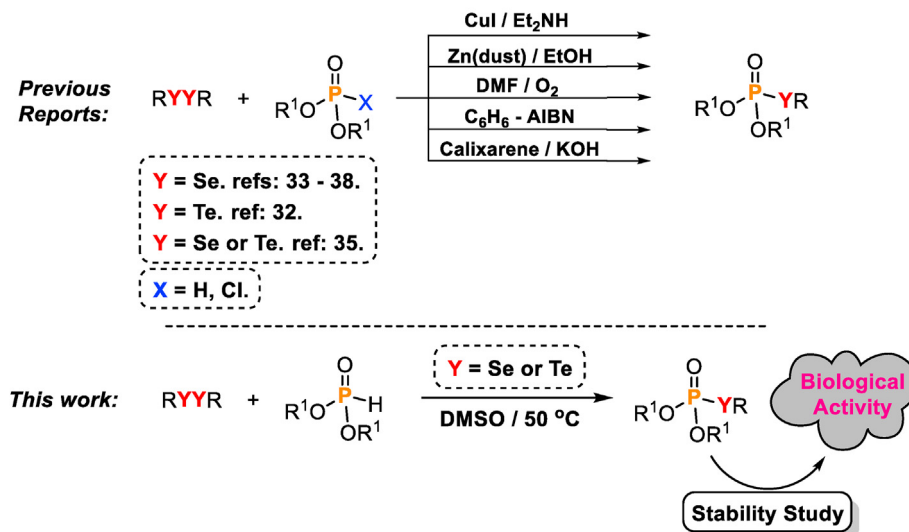
Organic chalcogen compounds have become versatile building blocks for organic synthesis [1–7], particularly under mild conditions [8–15]. Among the organic chalcogen compounds, phosphorochalcogenoates are important intermediates in organic synthesis [16–21] and can be an alternative route to access heterocyclic compounds [22]. In addition, there is an interest in phosphorochalcogenoate derivatives because of their numerous biological properties, especially those containing sulfur elements [23–25], and because of their similarities with the phosphate functional group [26–28]. Thus, a combination of the biological activities of chalcogen compounds [29–31] with phosphonate

groups could improve applications in agrochemical and pharmaceutical fields.

Distinctive methodologies have been developed to form Se–P(O) bond (Scheme 1) [32–39]. According to the literature, various synthetic protocols employ harsh conditions, as metals [32,35–37], bases [34,35,37], oxidant [38], radical specie, [33] and harmful organic solvents [32–34,38]. Additionally, the more recent method developed to form S–P(O) bond, the authors have reported the obtaining phosphoroselenoates using *H*-phosphonate and *N*-(phenylseleno)phthalimide as starting materials under solvent-free conditions, however, only two compounds are obtained [39]. Regarding the biological activity evaluation, Hajra and co-workers prepared phosphoroselenoates from diselenides and *H*-phosphonates using zinc (dust) in EtOH and evaluated their biological activity [36]. *In vitro* antimicrobial and antifungal evaluations demonstrated that these compounds possess relevant biological applications. This is the unique biological study carried out for

* Corresponding author.

E-mail addresses: lucielisavegnago@yahoo.com.br (L. Savegnago), silva.ms@ufpel.edu.br (M.S. Silva).



Scheme 1. Examples of the synthesis of phosphorochalcogenoates (Se and Te).

these phosphorochalcogenoates (Se), emphasizing the needs to improve the discernments about this organic class of compounds.

Although there is an ample number of methods for forming S–P(O) bond [40–47], a simple and rapid methodology for the synthesis of phosphorochalcogenoate (Se and Te) frameworks remains necessary. Moreover, the methodologies to access Se–P(O) and Te–P(O) bond formation involve metals, bases, harsh conditions and time-consuming methods, which decompose the phosphorochalcogenoates containing tellurium element due to their instability compared to selenium element. According to the literature only one synthetic procedure was able to prepare phosphorochalcogenoates using both elements (Se and Te), employing CuI and Et₂NH (Scheme 1) [35].

Based on the development of a greener and practical protocol with a greater substrate scope (Se and Te) to obtain phosphorochalcogenoates, and in terms of antioxidant activities of chalcogen compounds [29–31] and phosphorylated derivatives [48–53], we report a simple and rapid method for the synthesis of some novel Se- and Te-aryl and alkyl phosphorochalcogenoates using only DMSO as solvent at 50 °C, where neither catalyst nor additive is required. Moreover, the major limitation of these prepared compounds is the sensitivity to air, moisture, and harsh experimental conditions, which was accessed by the stability study, especially those containing tellurium atom. Furthermore, the results were extremely important to design the biological study, as antioxidant and radical scavenging activity, since byproducts from phosphorochalcogenoate compounds could interfere in biological assays, hampering the interpretation.

2. Results and discussion

2.1. Chemistry

We commenced optimization of the reaction conditions using diphenyl diselenide **1a** with dimethyl *H*-phosphonate **2a**. The reaction conditions were investigated as outlined in Table 1. Initially, the reaction was carried out using 0.25 mmol of **1a** with 0.125 mmol of **2a** in DMSO at 25 °C in the presence of KOH (0.05 mmol). After 7.5 h, the yield was just 69% (Table 1, entry 1). To our delight, when the reaction was performed without catalyst, product **3a** was obtained in 83% yield (Table 1, entry 2 vs 1). Although an excess of

diselenide **1a** was not effective in improving the reaction conditions, an excess of *H*-phosphonate **2a** increased the yield to 91% (Table 1, entry 3 vs 4). When the temperature was increased to 50 °C, yield increased to 97% in 2.0 h of reaction time (Table 1, entry 6). Reaction at 90 °C showed a significant decrease in yield when compared to the reaction at 50 °C (Table 1, entry 7 vs 6). Almost quantitative formation of the desired product **3a** in DMSO at 50 °C with no catalyst, base or oxidant was achieved after 2.0 h. Subsequently, other solvents were also evaluated, including H₂O, glycerol, THF, EtOH, MeCN, DMF and PEG-400 (Table 1, entries 8–14). No reaction occurred in H₂O, glycerol and THF as solvent (Table 1, entries 8–11). On the other hand, the use of MeCN, EtOH, DMF and PEG-400 proved to be efficient in obtaining product **3a**, but only after a long reaction time (Table 1, entries 11–14 vs 6). In solvent-free conditions the formation of product **3a** was not efficient (Table 1, entry 15). Then, aiming to decrease the time, the reaction was performed under ultrasound irradiation (US), and the expected product **3a** was obtained in 84% yield after 0.5 h (Table 1, entry 16).

Thus, the best reaction condition to prepare compound **3a** involve the stirring of a mixture of diphenyl diselenide **1a** (0.125 mmol) and dimethyl *H*-phosphonate **2a** (0.300 mmol) in DMSO (0.5 mL) as a solvent at 50 °C for 2.0 h in an open flask (Table 1, entry 6).

Next, we turned our attention to the reactional substrate scope (Scheme 2), evaluating different diselenides **1** and *H*-phosphonates **2** under optimized reaction conditions. The reaction provided phosphoroselenoates **3a–d** in excellent yield (93–98%), regardless of the steric effect of the *H*-phosphonate. Only in the case of a phenyl group (Scheme 2, product **3e**) was the reaction not effective, probably due to the lower basicity of the diphenyl *H*-phosphonate [54,55]. After evaluating the influence of the *H*-phosphonate substituents, the effect of the structure of the other starting material (diphenyl diselenide **1**) on the yield and reaction time was investigated. Several diaryl and dialkyl diselenides **3f–m** were employed, all with good to excellent yields (82–98%). The electronic nature of the substituents on the diaryl diselenide did not change the profile of the Se–P(O) bond formation (Scheme 2). However, when dinaphthyl diselenide was used only traces of the product were observed (Scheme 2, product **3l**).

To exemplify the full structural elucidation, ¹H, ¹³C{¹H}, ³¹P{¹H}, HSQC and HMBC NMR experiments were performed with the

Table 1
Optimization of the reaction conditions for the synthesis of phosphorochalcogenoate **3a**^a.

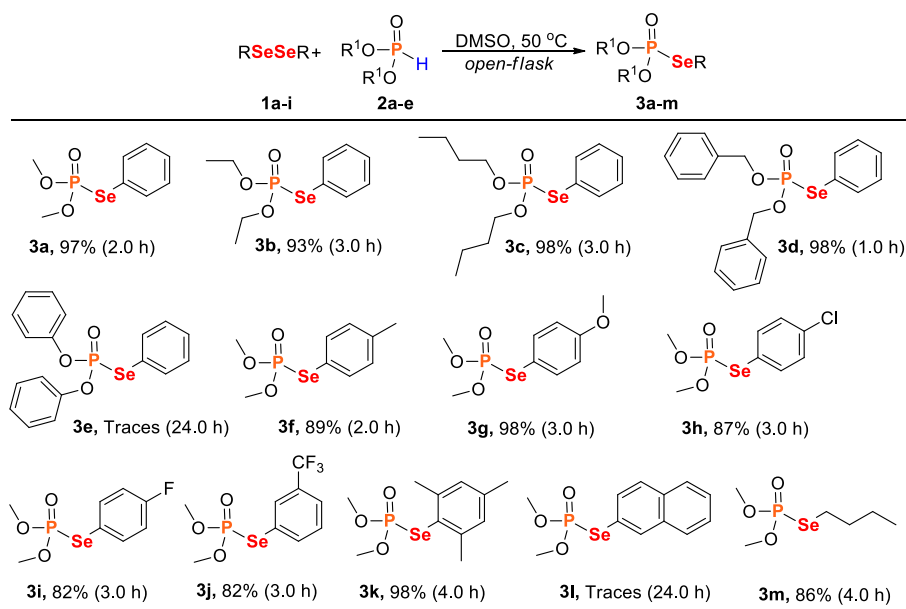
#	1 (mmol)	2 (mmol)	Solvent	Temperature (°C)	Time (h)	Yield (%) ^b
1 ^c	0.125	0.250	DMSO	25	7.5	69
2	0.125	0.250	DMSO	25	7.5	83
3	0.150	0.250	DMSO	25	7.5	70
4	0.125	0.300	DMSO	25	7.5	91
5	0.125	0.300	DMSO	30	7.5	91
6	0.125	0.300	DMSO	50	2.0	97
7	0.125	0.300	DMSO	90	2.0	67
8	0.125	0.300	H ₂ O	50	24.0	NR
9	0.125	0.300	Glycerol	50	24.0	NR
10	0.125	0.300	THF	50	24.0	NR
11	0.125	0.300	MeCN	50	24.0	61
12	0.125	0.300	EtOH	50	24.0	95
13	0.125	0.300	DMF	50	24.0	89
14	0.125	0.300	PEG-400	50	24.0	85
15	0.125	0.300	—	50	24.0	28
16 ^d	0.125	0.300	DMSO	—	0.5	84

^a Reactions performed using dimethyl *H*-phosphonate **1a**, diphenyl diselenide **2a** and solvent (0.5 mL) in an open flask.

^b Yields of isolated product.

^c Reaction performed using KOH (0.05 mmol).

^d Reaction performed with ultrasound energy; NR = no reaction.



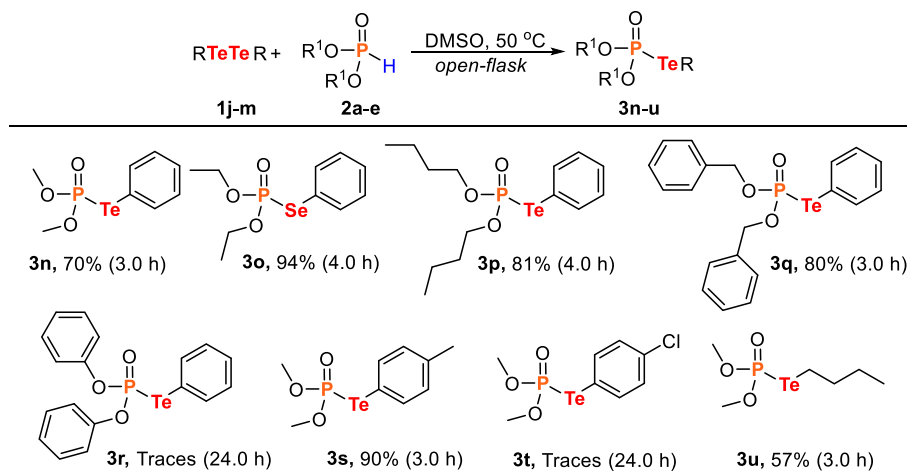
Scheme 2. Substrate scope for the synthesis of phosphoroselenoates **3a-m**.

product **3j**. As can be seen in the support information, ¹H NMR signals appear at $\delta_{\text{H}} = 3.82$ ppm (methyl groups), presenting a coupling constant with phosphorus atom ($J_{\text{H-P}} = 13.2$ Hz), and at aromatic region with a typical *meta*-substitution multiplicity. The ¹³C{¹H} NMR experiment showed eight signals with fluoride and phosphorus scalar couplings, which according to the HSQC NMR experiment was possible to designate the carbons attached to the protons. Based on the carbon-13 chemical shifts and HMBC NMR experiment the quaternary carbons were confirmed. Additionally, coupling constants with phosphorus atom were imperative to aid the structural characterization in all compounds prepared, such as the quaternary carbon bonded to the selenium atom in the product **3j** that demonstrates a coupling constant with phosphorus atom ($J_{\text{P-C}} = 2.5$ Hz).

After determining the substrate scope regarding substituted diorganyl diselenides, the effect of ditelluride **1j-m** on Te–P(O)

bond formation was explored (Scheme 3). On evaluating the *H*-phosphonates to obtain phosphorotelluroates **3n-u**, the result was similar to the diselenides (Scheme 3, 57–94%). Moreover, the reactivity of diphenyl *H*-phosphonate was also ineffective in obtaining Te–P(O) bond formation under optimized reaction conditions. The variation with ditelluride was less effective than with diselenide. As can be seen in Scheme 3, the yields decreased, and the substrate scope was limited. In addition, when diphenyl ditelluride with an electron withdrawing group in the phenyl group was used, only traces of the product were observed even after a long reaction time (Scheme 3, product **3t**).

The full structural characterization was also carried with phosphorotelluroates. Similar to selenium compounds elucidation, the ¹H NMR spectrum of product **3q** (SI) demonstrates a signal at $\delta_{\text{H}} = 5.08$ ppm with a scalar coupling with phosphorus atom ($J_{\text{H-P}} = 13.2$ Hz), and six signals at aromatic region. Considering the



Scheme 3. Substrate scope for the synthesis of phosphorotelluroates **3n-u**.

integral values, it was possible to discriminate the aromatic ring attached to the tellurium atom with benzyl aromatic rings in the ^1H NMR spectrum. The $^{13}\text{C}\{^1\text{H}\}$ NMR spectrum also shows coupling constants with phosphorus atom, which supports the carbons discrimination. HSQC and HMBC NMR experiments have confirmed the quaternary carbons. It is important to mention that the 2D NMR experiments were not performed for all compounds, since the scalar couplings with phosphorus atom provide useful data for structures elucidation.

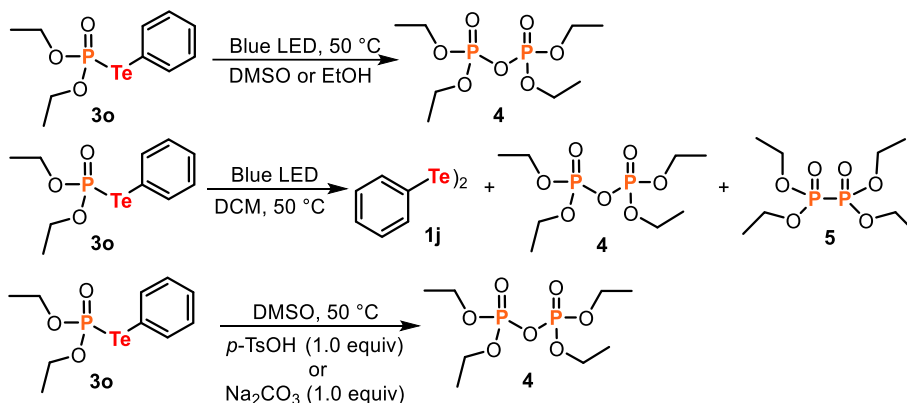
Based on the explored substrate scope, the experimental features of the reactions and the distinctive results obtained from the diselenide and ditelluride starting materials, we decided to verify the stability of these products. For this investigation phosphoroselenoate **3b** and phosphotelluroate **3o** were chosen as standard compounds. Product **3b** was stable in the presence of light (Blue LED) for 24.0 h in different solvents (DMSO, DCM and EtOH) and when submitted to acid (TsOH, 1.0 equiv) or base (Na_2CO_3 , 1.0 equiv) in DMSO solvent at 50 °C for 24.0 h it remained intact. These results emphasize the high stability of the Se–P(O) bonding and explain the greater number of methods for obtaining phosphoroselenoates (Scheme 1).

On the other hand, when phosphorotelluroate **3o** was investigated in the stability study, different by-products were identified (Scheme 4). Product **3o** is more reactive in the outlined conditions and by-products were formed in the presence of light in 2.0 h of reaction time. By-products **4** and **5** were identified by $^{31}\text{P}\{^1\text{H}\}$

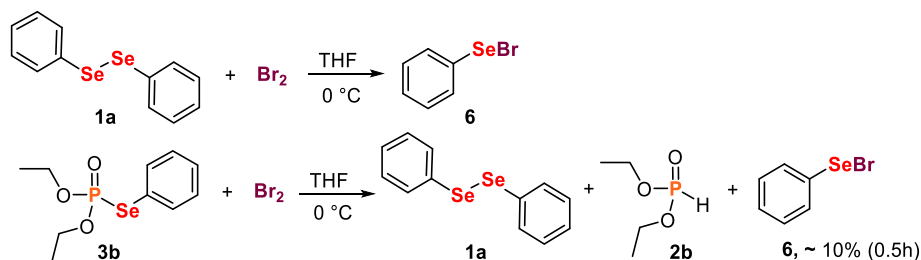
NMR, as given in the literature [56,57] and starting material **1j** was identified by $^{125}\text{Te}\{^1\text{H}\}$ NMR spectroscopy. In DCM solvent, product **3o** was less reactive but still observed in small amounts (~20%). In DMSO and EtOH solvents, product **3o** degrades completely and only by-product **4** was observed by $^{31}\text{P}\{^1\text{H}\}$ NMR spectroscopy. Diphenyl ditelluride **1j** was not detected, and we believe that it was transformed to tellurium oxide, as seen by the formation of a white solid. When acid or base media in DMSO at 50 °C were tested, only by-product **4** was observed, together with this white solid.

After demonstrating the stability of the products against light and acid–base media, we evaluated the Se–P(O) bond reactivity against molecular bromine. It is well-known that bromine reacts with diselenides to form reactive electrophiles (Scheme 5, Br–Se-Aryl**6**) [58]. When a THF solution of molecular bromine was added to a THF solution of phosphoroselenoate **3b** at 0 °C, the starting materials were obtained. The reactive electrophile phenylselenanyl bromide **4** was formed in around of 10% yield (Scheme 5). The products were confirmed by $^{31}\text{P}\{^1\text{H}\}$ and $^{77}\text{Se}\{^1\text{H}\}$ NMR spectroscopy (Figures 96S and 97S). Based on this result, it is possible to observe that Se–P(O) bonding is also labile but stronger than Te–P(O) bonding. On evaluating the stability of phosphorotelluroate **3o** against bromine to obtain the electrophile phenyltellanyl bromide, the result was the same as with phosphoroselenoate **3b** (SI).

Based on the stability studies we can conclude that the higher instability of phosphorotelluroates is because of the weak Te–P(O) bonding, which justified the small substrate scope obtained from



Scheme 4. Stability evaluation of phosphorotelluroate **3o** under different reaction conditions.

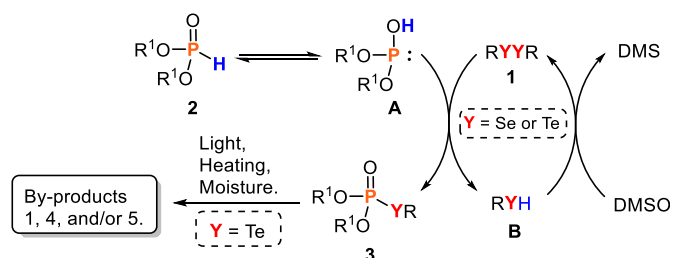


Scheme 5. Stability evaluation of phosphoroselenoate **3b** against molecular bromine.

diorganyl ditellurides in our procedure. In addition, the studies also suggest possible reasons why some of the protocols demonstrated in the literature (Scheme 1) to form phosphorotelluroates did not work. After evaluating the stability of the products, we decide to scale-up this protocol in an attempt to estimate the stability in a gram-scale reaction. The procedure was performed using 5 mmol of diethyl *H*-phosphonate **2b** with 2.1 mmol of diphenyl dichalcogenide **1a** or **1j** in DMSO at 50 °C. The yields obtained were comparable to the small-scale reactions, affording the products in **3b** and **3o** in 87% and 90%, respectively.

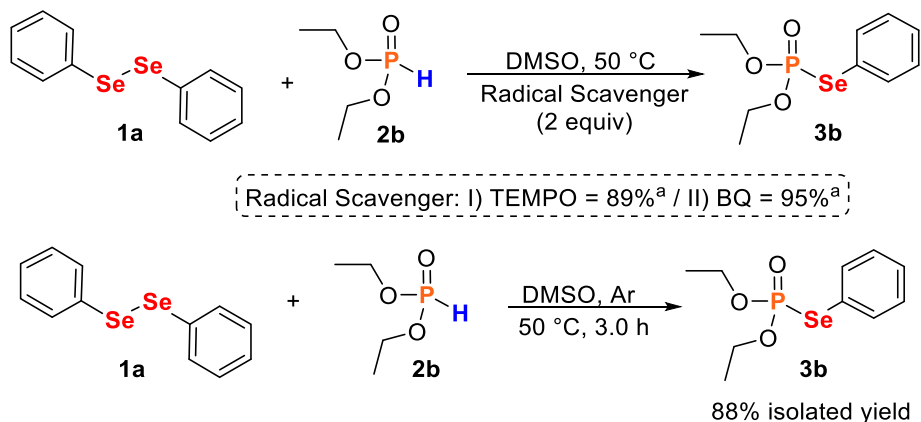
We have carried out some control experiments to investigate the mechanistic pathway to obtain phosphorochalcogenoates. Thus, when the reaction between diphenyl diselenide **1a** and *H*-phosphonate **2b** was performed in the presence of radical scavengers (2.0 equiv), including 2,2,6,6-tetramethyl-1-piperidinyloxy (TEMPO) and 1,4-benzoquinone (BQ), the yields stayed the same in 3.0 h of reaction time (Scheme 6). Therefore, these results clearly supported that the free radical mechanism was not involved in phosphorochalcogenoate formation. Then we performed a reaction under argon and observed that the yield was not affected by an inert atmosphere (Scheme 6).

On the basis of the control experiments and the scope profile of this procedure, a plausible mechanism was proposed (Scheme 7). Initially, tautomerization of the *H*-phosphonate occurs to form the intermediate **A**. The basicity of tautomer **A** is well-known [47,54] and reaction with dichalcogenides provides phosphorochalcogenoates. Furthermore, intermediate **B** is also formed, which is oxidized *in situ* to dichalcogenides for subsequent runs. This oxidation procedure reutilizes intermediate **B** and increases the atomic efficiency of the reaction. For phosphorotelluroate, instability hampers the reaction scope and some of these products degrade to by-products **4** and **5**, together with tellurium oxide.



Scheme 7. A plausible mechanistic pathway.

The greener synthetic procedure developed is desirable for pharmacological studies, since no catalyst and metal were employed, which avoids contaminations. Additionally, DMSO is a useful solvent because the application in chemical processes, and due the lower toxicity compared to hydrocarbons, and chlorinated solvents [59]. Overall, the substrate scope evaluation has provided the stability profile of the distinct phosphorochalcogenoates synthesized. In addition to the stability parameters accessed (light, solvent, and acid/base media), the substrate scope demonstrated that heating and long reaction-time were imperative to the decreasing of the yields. The phosphorotelluroates are not stable enough for biological evaluation, because the standard experimental conditions. The use of tellurium products could generate non-confident results. In this sense, the phosphoroselenoates were selected as the proper substrates for biological analyses. As can be seen in Scheme 2, the compounds **3a**, **3c**, **3d**, **3f**, **3g**, and were designated for the biological study due to their higher stability during the storage, and the structural distinction.



Scheme 6. Control experiments. ^a Yield of isolated product.

2.2. In vitro biological results

2.2.1. Thiobarbituric acid reactive species assay in brain total of mice

The levels of TBARS in the lipid peroxidation induced by SNP in cerebral tissue were reduced for compounds at different concentrations. As shown in Table 2, **3f** and **3d** compound were effective at concentration of 10 μ M, while the compounds **3c** and **3g** showed a significant inhibition of the lipid peroxidation at the concentration of 500 μ M. The **3a** compound was not effective in lowering TBARS levels.

2.2.2. Reactive species assay in brain total of mice

In this study was evaluated the capacity of the compounds in neutralizing the RS in cerebral tissue of mice (Table 3). The results from the RS assay demonstrate that compounds **3a** and **3d** decreased the formation of RS induced by azide in the cerebral tissue of mice at concentrations equal to or higher than 10 μ M, while **3c** and **3g** compounds were effective only at the concentration of 50 μ M and 100 μ M, respectively. The **3f** compound was not effective in neutralizing the RS in cerebral tissue of mice.

2.2.3. Ferric ion reducing antioxidant power

The FRAP assay was used to determine the reducing power of compounds to elucidate the relationship between the antioxidant effect and the reducing power (Table 4). Compounds **3c**, **3d**, **3f** and **3g** exhibited ferric-reducing ability at concentration of 500 μ M and **3a** compound did not present this power.

2.2.4. Radical scavenging activity

Table 5 demonstrates that the compounds **3a** and **3g** present a significant DPPH radical scavenging activity at concentrations 500 μ M, while the other compounds did not demonstrate radical scavenging efficiency.

Table 6 shows the antioxidant ability of **3a**, **3f** and **3g** compounds in ABTS + assay. The compound **3a** and **3f** were effective at concentrations equal to and higher than 50 μ M, while the **3g** presented radical scavenging efficiency at concentration equal to 500 μ M.

2.3. Ex vivo biological results

2.3.1. Thiobarbituric acid reactive species assay in brain, liver and kidney of mice

Table 7 demonstrates that the compounds **3f** and **3g** present antioxidant activity in the brains of mice at the dose of 10 mg/kg, while that in the liver and kidney none compounds presented activity. Interestingly, the **3a** compound presents pro-oxidant activity.

Table 2
Effect phosphoroselenoates on the TBARS assays in cerebral tissue of mice.

Compounds	Concentrations (μ M)			
	10	50	100	500
3a	84.69 \pm 8.41	80.59 \pm 11.5	85.89 \pm 7.34	79.77 \pm 4.97
3c	79.35 \pm 4.97	83.79 \pm 5.83	90.36 \pm 3.05	57.02 \pm 13.05 **
3d	59.51 \pm 14.15 *	—	—	—
3f	73.00 \pm 0.69 *	—	—	—
3g	87.64 \pm 2.42	78.64 \pm 2.68	78.11 \pm 0.72	57.96 \pm 8.95 ***

Data are expressed as mean \pm SEM (n = 3) of % of lipid peroxidation in cerebral tissue; Control: 33.50 \pm 5.65; Induced: 100; Trolox (10 μ M, positive control): 29.75 \pm 0.85. (* p < 0.05, ** p < 0.01 and *** p < 0.001) when compared to induced (100% of oxidation). One-way ANOVA followed by the Tukey.

Table 3
Effect phosphoroselenoates on reactive species production assays in the cerebral cortex of mice.

Compounds	Concentrations (μ M)			
	10	50	100	500
3a	71.50 \pm 13.00 *	—	—	—
3c	98.30 \pm 7.15	76.10 \pm 7.90 *	61.40 \pm 2.76 **	—
3d	61.70 \pm 15.00 *	—	—	—
3f	70.30 \pm 18.90	84.90 \pm 13.40	70.10 \pm 17.50	62.7 \pm 12.3
3g	94.00 \pm 11.10	94.10 \pm 3.92	67.20 \pm 15.80 *	—

Data are expressed as mean \pm SEM (n = 3) of units of fluorescence. Control: 82.10 \pm 0.05; Induced: 139.00 \pm 26.80; Trolox (10 μ M, positive control): 99 \pm 15.53. The letters represent significant difference (* p < 0.05 and ** p < 0.01) when compared to induced. One-way ANOVA followed by the Tukey.

Table 4
Effect phosphoroselenoates on the FRAP assay.

Compounds	Concentration (μ M)			
	10	50	100	500
3a	0.11 \pm 0.02	0.12 \pm 0.01	0.12 \pm 0.02	0.16 \pm 0.01
3c	0.11 \pm 0.02	0.15 \pm 0.01	0.15 \pm 0.01	0.3 \pm 0.01 ***
3d	0.16 \pm 0.01	0.23 \pm 0.04	0.40 \pm 0.03	1.02 \pm 0.18 ***
3f	0.14 \pm 0.01	0.17 \pm 0.016	0.17 \pm 0.04	0.29 \pm 0.04 *
3g	0.16 \pm 0.01	0.16 \pm 0.01	0.19 \pm 0.03	0.26 \pm 0.02 **

Data expressed mean \pm SEM (n = 3) of absorbance; Vehicle: 0.11 \pm 0.02; Trolox (10 μ M, positive control): 0.39 \pm 0.132. The letters represent significant (* p < 0.05, ** p < 0.01 and *** p < 0.001) when compared to vehicle. One-way ANOVA followed by the Tukey.

Table 5
Effect phosphoroselenoates on the DPPH radical scavenging.

Compounds	Concentration (μ M)			
	10	50	100	500
3a	5.53 \pm 3.67	7.83 \pm 4.09	4.68 \pm 2.39	21.93 \pm 0.88 *
3c	6.14 \pm 6.14	18.38 \pm 7.49	12.21 \pm 6.20	7.38 \pm 4.18
3d	2.19 \pm 2.19	3.94 \pm 3.94	3.72 \pm 3.72	5.04 \pm 5.04
3f	12.20 \pm 6.48	6.83 \pm 2.93	9.87 \pm 9.87	3.62 \pm 3.62
3g	3.72 \pm 3.72	6.95 \pm 3.81	11.92 \pm 4.69	19.06 \pm 3.60 *

Data expressed mean \pm SEM (n = 3) percentage of scavenging activity in relation to vehicle. Vehicle: 0.00 \pm 0.00; Trolox (10 μ M, positive control): 93.5 \pm 0.28. The letters represent significant difference (* p < 0.05) when compared to vehicle group. One-way ANOVA followed by the Tukey.

Table 6
Effect phosphoroselenoates on the ABTS⁺ radical scavenging.

Compounds	Concentration (μ M)			
	10	50	100	500
3a	5.02 \pm 3.19	10.35 \pm 1.09 *	—	—
3c	1.92 \pm 1.92	8.76 \pm 0.79	3.84 \pm 3.14	2.34 \pm 2.34
3d	3.85 \pm 3.85	3.06 \pm 3.06	1.86 \pm 0.93	12.40 \pm 6.53
3f	11.50 \pm 1.22	12.50 \pm 2.64	29.90 \pm 1.92 ***	—
3g	6.76 \pm 2.59	8.60 \pm 2.43	6.91 \pm 3.29	19.80 \pm 2.57 **

Data expressed mean \pm SEM (n = 3) percentage of scavenging activity in relation to vehicle. Vehicle: 0.00 \pm 0.00; Trolox (10 μ M, positive control): 94.33 \pm 2.60. The letters represent significant difference (* p < 0.05 ** p < 0.01 *** p < 0.001) when compared with vehicle group. One-way ANOVA followed by the Tukey.

2.3.2. SOD and GPx activity in brain of mice

As seen in Table 8, the compounds **3a**, **3c** and **3g**, at the dose of 10 mg/kg, decreased the activity of GPx, and **3f** and **3g** decreased the activity of SOD. **3d** did not demonstrate any effect.

Table 7Effect of **3a**, **3c**, **3d**, **3f** and **3g** (10 mg/kg) on lipid peroxidation in the brain, liver and kidney mice.

Compounds	TBARS in the brain	TBARS in the liver	TBARS in the kidney
Control	91.91 ± 9.38	271.5 ± 43.88	438.20 ± 27.59
3a	87.34 ± 13.19	326.0 ± 11.72	676.60 ± 80.76*
3c	87.71 ± 18.57	249.40 ± 44.63	371.00 ± 27.89
3d	83.00 ± 11.89	263.80 ± 24.2	580.5 ± 66.58
3f	54.79 ± 7.41*	199.90 ± 39.95	455.4 ± 32.70
3g	64.64 ± 7.63*	280.80 ± 65.93	422.5 ± 81.08

Data are reported as mean ± SEM of 6 animals per group. (*) denotes p < 0.05 as compared to the control group (canola oil); (the Student's t-test).^a TBARS levels/g tissue.**Table 8**Effect of **3a**, **3c**, **3d**, **3f** and **3g** (10 mg/kg) on SOD and GPx activity in the brain of mice.

Compounds	GPx ^a	SOD ^b
Control	12.8 ± 2.28	25.44 ± 4.12
3a	7.18 ± 2.86*	25.94 ± 5.22
3c	5.50 ± 1.35*	23.85 ± 1.84
3d	6.39 ± 1.55	17.54 ± 0.91
3f	7.48 ± 2.78	7.37 ± 0.46**
3g	4.98 ± 0.61**	13.47 ± 2.89*

Data are reported as mean ± SEM of 6 animals per group. (*) denotes p < 0.05 and (**) denotes p < 0.01 as compared to the control group (canola oil); (the Student's t-test).^a nmolNADPH/g tissue; ^b units/min.

2.3.3. Toxicological parameters

Table 9 demonstrates that, at the dose of 10 mg/kg, **3g** decreased plasma urea and increased plasma creatinine. None of the compounds at the dose of 10 mg/kg altered alanine aminotransferase (ALT) and aspartate aminotransferase (AST) plasma levels.

Data are reported as mean ± SEM of 5/6 animals per group. (*) denotes p < 0.05 and (***) denotes p < 0.001 as compared to the control group; (the Student's t-test).^a mg/dL; ^b IU/L.

2.4. Biological discussion

The antioxidant potential of phosphoroselenoates compounds was investigated because the involvement of oxidative stress has been attributed in a variety of human diseases. Thus, the **3a**, **3c**, **3d**, **3f** and **3g** compounds were tested *in vitro* and *ex vivo* for the antioxidant potential, as well as to investigation toxicity in mice through of the plasma levels of markers of renal and hepatic damage. The results of the present study demonstrate that the phosphoroselenoates compounds had an *in vitro* antioxidant activity, in addition, the **3a**, **3c**, **3f** and **3g** compounds, at dose 10 mg/kg, presented *ex vivo* antioxidant activity. It is noteworthy that the compounds not caused changes in plasma markers of renal and hepatic damage in mice, only the compound **3g** increased the creatinine levels, but more studies are necessary to investigate this change.

Table 9Plasma toxicological parameters of hepatic and renal damage of **3a**, **3c**, **3d**, **3f** and **3g** (10 mg/kg) on mice.

Compounds	Urea ^a	Creatinine ^a	AST ^b	ALT ^b
Control	90.31 ± 0.74	1.77 ± 0.05	148.00 ± 8.08	110.90 ± 12.4
3a	80.30 ± 6.54	1.78 ± 0.15	151.20 ± 4.50	117.40 ± 4.94
3c	105.00 ± 3.94	1.75 ± 0.27	159.30 ± 4.07	140.00 ± 7.86
3d	98.59 ± 5.91	1.52 ± 0.18	155.30 ± 2.66	138.10 ± 8.55
3f	80.24 ± 9.80	1.96 ± 0.22	147.40 ± 9.75	119.00 ± 4.49
3g	74.39 ± 1.78***	2.36 ± 0.18*	151.00 ± 5.07	119.50 ± 4.26

In vitro, phosphoroselenoates protected against lipid peroxidation induced by SNP and reactive species induced by SNP in mice brain homogenate. The mechanism of action by which phosphoroselenoates shows antioxidant activity is related to its DPPH and ABTS + -scavenging activity as well as reducing power of iron. Based on the *in vitro* results, we expanded the study to investigate the effect of oral administration of compounds. It was demonstrated that **3f** and **3g** compounds decreased the oxidative stress parameters in the brains of mice and the **3f** reduced the lipid peroxidation levels and decreased the SOD and GPx activities. The results indicate that a reduction of reactive species, could decrease the SOD activity and consequently it causes decrease of GPx activity. The compounds **3a**, **3c** and **3g** altered the antioxidant enzymes, that can be a mechanism to neutralize oxidative stress, because the SOD catalyzes the dismutation of superoxide into oxygen and hydrogen peroxide. The compounds affected only the brain, probably because this organ contains a high degree of polyunsaturated fatty acids, substrates particularly vulnerable to oxidation, and is rich in non-haem iron, which is catalytically involved in the generation of free radicals [60].

Recently studies proved that phosphorus-containing compounds increase the pharmacokinetics propriety of drugs [61]. Thus, organoselenium compounds could have their proprieties improved by adding a phosphorus molecule in their structures. Furthermore, a new study on phosphorus supply and selenium uptake on plants [62] shows that increase supply of P enhances Se transportation across the cell membrane raising the availability of selenium in the cell, as a result the new selenium availability inside the cell could be used to the formation of enzymes and selenoproteins used in the antioxidant system [63].

Basal levels of reactive oxygen species and reactive nitrogen species are physiologically produced by many mechanisms, including oxidative deamination of biogenic amines and reduction of O₂ via mitochondrial electron transport chain [64,65]. However, when there is an imbalance between the production of reactive species and the natural antioxidant defenses result in oxidative stress [66]. There is some evidence that reactive species, including superoxide anion, hydrogen peroxide and singlet oxygen, play an important role in the pathogenesis of cancer, neurodegeneration, and psychiatric disorders as well as aging [67,68]. For this reason, these compounds may be used as synthetic antioxidants that provide protection in pathologies related to oxidative stress including diabetes, cardiovascular diseases, cancer, and several neurodegenerative diseases. In addition, we can highlight the compound **3g**, which in addition to presenting good to excellent yields (98%), also showed promising antioxidant effect, both *in vitro* and *ex vivo* assay, this may be due to its chemical structure presenting methoxyphenyl group, because the methoxyphenyl derived compounds usually exhibit a series of pharmacological properties such as anticancer [69], antioxidant [69], antibacterial [70], and analgesic [71]. However, **3g** compound (10 mg/kg) increased plasma levels of creatinine in the blood of mice, therefore, in future studies should be investigated the toxicity of this compound and check if at lower doses will have a promising antioxidant effect without causing changes in the markers of kidney damage, we point out that this was a limitation of this study.

3. Conclusions

In summary, a simple and efficient protocol for the formation of Se–P(O) and Te–P(O) bonds from dichalcogenides and H-phosphonate was developed under catalyst-, and base-free conditions. The methodology provided a greener alternative to generate valuable chalcogen phosphonates *via* a rapid procedure. Full structural assignment and a stability evaluation of products were performed

for an effective operational description of this simple and feasible method. The stability study was vital to design the substrate scope for pharmacological activity. According to the biological studies, we could conclude that the phosphoroselenoates present antioxidant effect in different assays and these compounds are effective to act against oxidative stress in biological systems.

4. Experimental section

4.1. Chemistry

4.1.1. General information

The reactions were monitored by TLC carried out on Merck silica gel (60 F₂₅₄) by using UV light as visualizing agent and 5% vanillin in 10% H₂SO₄ and heat as developing agents. Baker silica gel (particle size 0.040–0.063 mm) was used for flash chromatography. Hydrogen nuclear magnetic resonance spectra (¹H NMR) were obtained on Bruker Avance III HD 400 MHz employing a direct broadband probe. Spectra were recorded in CDCl₃ solutions. Chemical shifts are reported in ppm, referenced to tetramethylsilane (TMS) as the external reference. Coupling constant (*J*) are reported in Hertz. Abbreviations to denote the multiplicity of a particular signal are s (singlet), d (doublet), dd (doublet of doublet), dt (doublet of triplet), t (triplet), td (triplet of doublet), quint (quintet), sex (sextet) and m (multiplet). Carbon-13 nuclear magnetic resonance spectra (¹³C NMR) were obtained on Bruker Avance III HD 400 MHz employing a direct broadband probe. Chemical shifts are reported in ppm, referenced to the solvent peak of CDCl₃. Coupling constant (*J*) are reported in Hertz. Abbreviations to denote the multiplicity of a particular signal are d (doublet), dd (doublet of doublet), q (quartet), qd (quartet of doublet) and m (multiplet). Phosphorus-31 nuclear magnetic resonance spectra (³¹P NMR) were obtained on Bruker Avance III HD 400 MHz employing a direct broadband probe. Spectra were recorded in CDCl₃ solutions. Chemical shifts are reported in ppm, referenced to triphenylphosphate (TPP). Coupling constant (*J*) are reported in Hertz. Abbreviations to denote the multiplicity of a particular signal are quint (quintet), sept (septet) and sept d (septet of doublet). Selenium-77 nuclear magnetic resonance spectra (⁷⁷Se NMR) were obtained on Bruker Avance III HD 400 MHz employing a direct broadband probe. Spectra were recorded in CDCl₃ solutions. Chemical shifts are reported in ppm, referenced to the diphenyl diselenide (462 ppm). Coupling constant (*J*) are reported in Hertz. Abbreviations to denote the multiplicity of a particular signal are d (doublet) and d quint (doublet of quintet). Tellurium-125 nuclear magnetic resonance spectra (¹²⁵Te NMR) were obtained on Bruker Avance III HD 400 MHz employing a direct broadband probe. Spectra were recorded in CDCl₃ solutions. Chemical shifts are reported in ppm, referenced to diphenyl ditelluride (422 ppm). Coupling constant (*J*) are reported in Hertz. Abbreviations to denote the multiplicity of a particular signal are d (doublet) and d quint (doublet of quintet). Fluorine-19 nuclear magnetic resonance spectra (¹⁹F NMR) were obtained on Bruker Avance III HD 400 MHz employing a direct broadband probe. Spectra were recorded in CDCl₃ solutions. Chemical shifts are reported in ppm, referenced to α,α,α -trifluorotoluene (–63.72 ppm). Coupling constant (*J*) are reported in Hertz. Abbreviations to denote the multiplicity of a particular signal is m (multiplet). Low-resolution mass spectra (MS) were obtained with a Shimadzu GC-MS-QP2010 mass spectrometer. The high-resolution mass spectrometry (QTOF) analysis was performed on a Bruker Daltonics micrOTOF-Q II instrument in operating positive mode. The samples were solubilized in HPLC-grade acetonitrile and injected into APCI source by means of a syringe pump at a flow rate of 5.0 μ L min⁻¹. The follow instrument parameters were applied: capillary and cone voltages were set to +3500 V and –500 V,

respectively, with a desolvation temperature of 180 °C. For data acquisition, processing and isotopes simulations, Compass 1.3 for micrOTOF-Q II software (Bruker daltonics, USA) was used. Melting point (mp) values were measured in a Marte PFD III instrument with a 0.1 °C precision.

4.1.2. General procedure for chalcogen (Se and Te)-phosphorus bond formation

The corresponding *H*-phosphonate (0.3 mmol), dichalcogenide (0.125 mmol) and DMSO (0.5 mL) were put into an open glass tube. The mixture was stirred at 50 °C for 1–4 h. After the reaction was complete, 10.0 mL of water was added. The mixture was extracted with ethyl acetate (3 × 10.0 mL). The combined organic layer was dried over MgSO₄ and evaporated in vacuo. The residue was purified by silica gel column chromatography to give the corresponding phosphorochalcogenoates **3**.

4.1.2.1. *O,O*-dimethyl *Se*-phenyl phosphoroselenoate (3a) [38]. Yield: 0.0645 g (97%); Yellowish oil. ¹H NMR (400 MHz, CDCl₃) δ (ppm) = 7.58–7.56 (m, 2H); 7.32–7.20 (m, 3H); 3.72 (d, *J*_{H-P} = 13.1 Hz, 6H). ¹³C-{¹H} NMR (100 MHz, CDCl₃) δ (ppm) = 135.6 (d, *J*_{C-P} = 4.6 Hz), 129.5 (d, *J*_{C-P} = 2.1 Hz), 128.9 (d, *J*_{C-P} = 2.6 Hz), 123.2 (d, *J*_{C-P} = 8.5 Hz), 53.9 (d, *J*_{C-P} = 5.6 Hz). ³¹P NMR (162 MHz, CDCl₃) δ (ppm) = 21.9 (sept, *J*_{P-H} = 13.1 Hz). ⁷⁷Se-{¹H} NMR (76 MHz, CDCl₃) δ (ppm) = 244.1 (d, *J*_{Se-P} = 490.5 Hz). IR (cm⁻¹): 2994, 2865, 1484, 1456, 1238, 1012, 854, 736. MS: *m/z* (rel. int., %) 266 (M⁺, 27.7), 157 (10.2), 109 (100.0), 79 (16.8), 77 (17.5), 51 (7.5). HRMS (APCI-QTOF) calculated mass for C₈H₁₁O₃PSe [M+H]⁺: 266.9689, found: 266.9686.

4.1.2.2. *O,O*-diethyl *Se*-phenyl phosphoroselenoate (3 b). [37] Yield: 0.0684 g (93%); Yellow oil. ¹H NMR (400 MHz, CDCl₃) δ (ppm) = 7.57 (d, *J* = 7.6 Hz, 2H); 7.30–7.22 (m, 3H); 4.18–4.03 (m, 4H); 1.23 (t, *J* = 7.1 Hz, 6H). ¹³C-{¹H} NMR (100 MHz, CDCl₃) δ (ppm) = 135.4 (d, *J*_{C-P} = 4.6 Hz), 129.4 (d, *J*_{C-P} = 1.9 Hz), 128.7 (d, *J*_{C-P} = 2.4 Hz), 123.7 (d, *J*_{C-P} = 8.4 Hz), 63.7 (d, *J*_{C-P} = 6.0 Hz), 15.8 (d, *J*_{C-P} = 7.3 Hz). ³¹P NMR (162 MHz, CDCl₃) δ (ppm) = 18.0 (quint, *J*_{P-H} = 9.0 Hz). ⁷⁷Se-{¹H} NMR (76 MHz, CDCl₃) δ (ppm) = 263.8 (d, *J*_{Se-P} = 480.6 Hz). IR (cm⁻¹): 2988, 2821, 1484, 1479, 1271, 986, 854, 744, 713. MS: *m/z* (rel. int., %) 294 (M⁺, 32.8), 238 (6.5), 158 (32.0), 137 (25.9), 109 (100.0), 81 (39.7), 77 (28.7), 51 (10.2). HRMS (APCI-QTOF) calculated mass for C₁₀H₁₅O₃PSe [M+H]⁺: 295.0002, found: 295.010.

4.1.3. *O,O*-dibutyl *Se*-phenyl phosphoroselenoate (3c)

[38] Yield: 0.0858 g (98%); Yellowish oil. ¹H NMR (400 MHz, CDCl₃) δ (ppm) = 7.59–7.56 (m, 2H); 7.29–7.21 (m, 3H); 4.08–3.97 (m, 4H); 1.55 (quint, *J* = 7.4 Hz, 4H); 1.27 (sex, *J* = 7.4 Hz, 4H); 0.82 (t, *J* = 7.4 Hz, 6H). ¹³C-{¹H} NMR (100 MHz, CDCl₃) δ (ppm) = 135.4 (d, *J*_{C-P} = 4.7 Hz), 129.3 (d, *J*_{C-P} = 1.9 Hz), 128.6 (d, *J*_{C-P} = 2.3 Hz), 123.7 (d, *J*_{C-P} = 8.4 Hz), 67.4 (d, *J*_{C-P} = 6.4 Hz), 31.9 (d, *J*_{C-P} = 7.2 Hz), 18.5, 13.4. ³¹P NMR (162 MHz, CDCl₃) δ (ppm) = 18.0 (quint, *J*_{P-H} = 8.0 Hz). ⁷⁷Se-{¹H} NMR (76 MHz, CDCl₃) δ (ppm) = 263.4 (d, *J*_{Se-P} = 478.5 Hz). IR (cm⁻¹): 2967, 2869, 1576, 1434, 1258, 1019, 740, 534. MS: *m/z* (rel. int., %) 350 (M⁺, 23.9), 294 (17.4), 238 (88.6), 158 (45.6), 137 (50.7), 77 (27.5), 57 (100.0), 55 (20.8), 51 (9.2), 41 (52.8). HRMS (APCI-QTOF) calculated mass for C₁₄H₂₃O₃PSe [M+H]⁺: 351.0628, found: 351.0643.

4.1.4. *O,O*-dibenzyl *Se*-phenyl phosphoroselenoate (3d)

[38] Yield: 0.1024 g (98%); Orange solid; m.p. = 75.4–77.8 °C. ¹H NMR (400 MHz, CDCl₃) δ (ppm) = 7.48 (d, *J* = 7.7 Hz, 2H); 7.28–7.14 (m, 13H); 5.08–4.99 (m, 4H). ¹³C-{¹H} NMR (100 MHz, CDCl₃) δ (ppm) = 135.8 (d, *J*_{C-P} = 4.5 Hz), 135.2 (d, *J*_{C-P} = 7.8 Hz), 129.4 (d, *J*_{C-P} = 1.9 Hz), 128.8 (d, *J*_{C-P} = 2.5 Hz), 128.5 (d, *J*_{C-P} = 2.3 Hz), 128.0, 123.2 (d, *J*_{C-P} = 8.5 Hz), 69.1 (d, *J*_{C-P} = 6.1 Hz). ³¹P NMR (162 MHz,

CDCl_3 δ (ppm) = 18.6 (quint, $J_{\text{P-H}} = 8.0$ Hz). $^{77}\text{Se}\{-^1\text{H}\}$ NMR (76 MHz, CDCl_3) δ (ppm) = 275.0 (d, $J_{\text{Se-P}} = 495.1$ Hz). IR (cm^{-1}): 2984, 2892, 2823, 1465, 1291, 986, 747, 702. MS: m/z (rel. int., %) 418 (M^+ , 2.3), 248 (5.4), 91 (100.0), 77 (7.2), 65 (14.3), 51 (4.8). HRMS (APCI-QTOF) calculated mass for $\text{C}_{20}\text{H}_{19}\text{O}_3\text{PSe} [\text{M}+\text{H}]^+$: 419.0315, found: 419.0324.

4.1.5. *O,O*-dimethyl *Se*-(*p*-tolyl) phosphoroselenoate (3f)

[33] Yield: 0.0623 g (89%); Yellow oil. ^1H NMR (400 MHz, CDCl_3) δ (ppm) = 7.51 (dd, $J = 8.0$ and 1.6 Hz, 2H); 7.12 (d, $J = 7.9$ Hz, 2H); 3.78 (d, $J_{\text{H-P}} = 13.1$ Hz, 6H); 2.34 (s, 3H). $^{13}\text{C}\{-^1\text{H}\}$ NMR (100 MHz, CDCl_3) δ (ppm) = 139.1 (d, $J_{\text{C-P}} = 2.9$ Hz), 135.6 (d, $J_{\text{C-P}} = 4.3$ Hz), 130.3 (d, $J_{\text{C-P}} = 2.1$ Hz), 119.3 (d, $J_{\text{C-P}} = 8.7$ Hz), 53.8 (d, $J_{\text{C-P}} = 5.6$ Hz), 21.1. ^{31}P NMR (162 MHz, CDCl_3) δ (ppm) = 22.3 (sept, $J_{\text{P-H}} = 13.1$ Hz). $^{77}\text{Se}\{-^1\text{H}\}$ NMR (76 MHz, CDCl_3) δ (ppm) = 234.4 (d, $J_{\text{Se-P}} = 495.6$ Hz). IR (cm^{-1}): 2990, 2859, 1495, 1449, 1210, 1029, 802, 731. MS: m/z (rel. int., %) 279 (M^+ , 37.1), 171 (11.3), 109 (100.0), 91 (40.0), 79 (17.3), 65 (8.9). HRMS (APCI-QTOF) calculated mass for $\text{C}_9\text{H}_{13}\text{O}_3\text{PSe} [\text{M}+\text{H}]^+$: 280.9846, found: 280.9840.

4.1.6. *Se*-(4-methoxyphenyl) *O,O*-dimethyl phosphoroselenoate (3g)

Yield: 0.0725 g (98%); Yellow oil. ^1H NMR (400 MHz, CDCl_3) δ (ppm) = 7.52 (dd, $J = 8.7$ and 1.9 Hz, 2H); 6.85 (d, $J = 8.7$ Hz, 2H); 3.80 (s, 6H); 3.77 (s, 3H). $^{13}\text{C}\{-^1\text{H}\}$ NMR (100 MHz, CDCl_3) δ (ppm) = 160.4 (d, $J_{\text{C-P}} = 2.6$ Hz), 137.3 (d, $J_{\text{C-P}} = 4.1$ Hz), 115.3 (d, $J_{\text{C-P}} = 2.3$ Hz), 112.9 (d, $J_{\text{C-P}} = 8.7$ Hz), 55.2, 53.9 (d, $J_{\text{C-P}} = 5.8$ Hz). ^{31}P NMR (162 MHz, CDCl_3) δ (ppm) = 22.3 (sept, $J_{\text{P-H}} = 13.0$ Hz). $^{77}\text{Se}\{-^1\text{H}\}$ NMR (76 MHz, CDCl_3) δ (ppm) = 230.6 (d, $J_{\text{Se-P}} = 500.7$ Hz). IR (cm^{-1}): 2995, 2866, 1492, 1428, 1256, 1008, 880, 719. MS: m/z (rel. int., %) 295 (M^+ , 57.1), 263 (10.4), 187 (26.7), 121 (9.1), 109 (100.0), 79 (16.0), 63 (10.8), 43 (2.8). HRMS (APCI-QTOF) calculated mass for $\text{C}_9\text{H}_{13}\text{O}_4\text{PSe} [\text{M}+\text{H}]^+$: 296.9795, found: 296.9796.

4.1.7. *Se*-(4-chlorophenyl) *O,O*-dimethyl phosphoroselenoate (3h)

[38] Yield: 0.0652 g (87%); Yellow oil. ^1H NMR (400 MHz, CDCl_3) δ (ppm) = 7.57 (dd, $J = 8.5$ and 1.9 Hz, 2H); 7.29 (d, $J = 8.5$ Hz, 2H); 3.80 (d, $J_{\text{H-P}} = 13.2$ Hz, 6H). $^{13}\text{C}\{-^1\text{H}\}$ NMR (100 MHz, CDCl_3) δ (ppm) = 136.8 (d, $J_{\text{C-F}} = 4.5$ Hz), 135.5 (d, $J_{\text{C-F}} = 3.0$ Hz), 129.7 (d, $J_{\text{C-F}} = 2.1$ Hz), 121.3 (d, $J_{\text{C-F}} = 8.7$ Hz), 54.0 (d, $J_{\text{C-F}} = 5.9$ Hz). ^{31}P NMR (162 MHz, CDCl_3) δ (ppm) = 21.2 (sept, $J_{\text{P-H}} = 13.2$ Hz). $^{77}\text{Se}\{-^1\text{H}\}$ NMR (76 MHz, CDCl_3) δ (ppm) = 243.3 (d, $J_{\text{Se-P}} = 483.0$ Hz). IR (cm^{-1}): 2987, 2891, 1502, 1471, 1227, 1018, 851, 730. MS: m/z (rel. int., %) 299 (M^+ , 17.1), 190 (5.4), 156 (7.2), 109 (100.0), 79 (13.8), 47 (2.2). HRMS (APCI-QTOF) calculated mass for $\text{C}_8\text{H}_{10}\text{ClO}_3\text{PSe} [\text{M}+\text{H}]^+$: 300.9300, found: 300.9299.

4.1.8. *Se*-(4-fluorophenyl) *O,O*-dimethyl phosphoroselenoate (3i)

Yield: 0.0682 g (96%); Yellow oil. ^1H NMR (400 MHz, CDCl_3) δ (ppm) = 7.64–7.60 (m, 2H); 7.03 (t, $J = 8.6$ Hz, H); 3.80 (d, $J_{\text{H-P}} = 13.2$ Hz, 6H). $^{13}\text{C}\{-^1\text{H}\}$ NMR (100 MHz, CDCl_3) δ (ppm) = 163.3 (dd, $J_{\text{C-F/C-P}} = 248.2$ and 2.9 Hz), 137.7 (dd, $J_{\text{C-F/C-P}} = 8.1$ and 4.3 Hz), 117.7 (dd, $J_{\text{C-P/C-F}} = 8.7$ and 3.5 Hz), 116.8 (dd, $J_{\text{C-F/C-P}} = 21.8$ and 2.2 Hz), 54.0 (d, $J_{\text{C-P}} = 5.8$ Hz). ^{31}P NMR (162 MHz, CDCl_3) δ (ppm) = 21.5 (sept d, $J_{\text{P-H/P-F}} = 13.1$ and 4.2 Hz); $^{77}\text{Se}\{-^1\text{H}\}$ NMR (76 MHz, CDCl_3) δ (ppm) = 239.8 (d, $J_{\text{Se-P}} = 486.7$ Hz). ^{19}F NMR (376 MHz, CDCl_3) δ (ppm) = -111.66 to -111.75 (m). IR (cm^{-1}): 3007, 2979, 1515, 1489, 1455, 1276, 1041, 899, 764. MS: m/z (rel. int., %) 284 (M^+ , 18.7), 175 (10.4), 109 (100.0), 95 (5.8), 79 (16.5), 57 (3.0). HRMS (APCI-QTOF) calculated mass for $\text{C}_8\text{H}_{10}\text{FO}_3\text{PSe} [\text{M}+\text{H}]^+$: 284.9595, found: 284.9597.

4.1.9. *O,O*-dimethyl *Se*-(3-(trifluoromethyl)phenyl) phosphoroselenoate (3j)

[38] Yield: 0.0685 g (82%); Yellow oil. ^1H NMR (400 MHz, CDCl_3)

δ (ppm) = 7.90 (s, 1H); 7.85 (d, $J = 7.7$ Hz, 1H); 7.63 (d, $J = 7.8$ Hz, 1H); 7.46 (t, $J = 7.8$ Hz, 1H), 3.82 (d, $J_{\text{H-P}} = 13.2$ Hz, 6H). $^{13}\text{C}\{-^1\text{H}\}$ NMR (100 MHz, CDCl_3) δ (ppm) = 138.8 (d, $J_{\text{C-P}} = 4.1$ Hz), 132.3–132.0 (m), 131.8 (qd, $J_{\text{C-F/C-P}} = 32.3$ and 2.5 Hz), 129.9 (d, $J_{\text{C-P}} = 1.6$ Hz), 125.8–125.7 (m), 124.4 (d, $J_{\text{C-P}} = 8.6$ Hz), 123.4 (q, $J_{\text{C-F}} = 271.2$ Hz), 54.1 (d, $J_{\text{C-P}} = 5.8$ Hz). ^{31}P NMR (162 MHz, CDCl_3) δ (ppm) = 20.7 (sept, $J_{\text{P-H}} = 13.2$ Hz). $^{77}\text{Se}\{-^1\text{H}\}$ NMR (76 MHz, CDCl_3) δ (ppm) = 255.9 (d, $J_{\text{Se-P}} = 475.1$ Hz). IR (cm^{-1}): 3031, 2945, 1534, 1476, 1242, 1050, 901, 793.

4.1.10. *Se*-mesityl *O,O*-dimethyl phosphoroselenoate (3k)

Yield: 0.0755 g (98%); Yellow oil. ^1H NMR (400 MHz, CDCl_3) δ (ppm) = 6.95 (s, 2H); 3.72 (d, $J_{\text{H-P}} = 12.7$ Hz, 6H); 2.56 (s, 6H); 2.26 (s, 3H). $^{13}\text{C}\{-^1\text{H}\}$ NMR (100 MHz, CDCl_3) δ (ppm) = 143.7 (d, $J_{\text{C-P}} = 3.9$ Hz), 139.4 (d, $J_{\text{C-P}} = 3.7$ Hz), 128.9 (d, $J_{\text{C-P}} = 3.1$ Hz), 121.2 (d, $J_{\text{C-P}} = 9.2$ Hz), 53.9 (d, $J_{\text{C-P}} = 7.0$ Hz), 24.7, 20.8. ^{31}P NMR (162 MHz, CDCl_3) δ (ppm) = 20.6 (sept, $J_{\text{P-H}} = 12.7$ Hz). $^{77}\text{Se}\{-^1\text{H}\}$ NMR (76 MHz, CDCl_3) δ (ppm) = 150.1 (d, $J_{\text{Se-P}} = 513.9$ Hz). IR (cm^{-1}): 2949, 2823, 1462, 1398, 1222, 987, 889, 802. MS: m/z (rel. int., %) 307 (M^+ , 15.2), 198 (15.8), 119 (100.0), 109 (6.0), 91 (13.2), 77 (5.6), 41 (2.8). HRMS (APCI-QTOF) calculated mass for $\text{C}_{11}\text{H}_{17}\text{O}_3\text{PSe} [\text{M}+\text{H}]^+$: 309.0159, found: 309.0155.

4.1.11. *Se*-butyl *O,O*-dimethyl phosphoroselenoate (3m)

[38] Yield: 0.0589 g (86%); Yellowish oil. ^1H NMR (400 MHz, CDCl_3) δ (ppm) = 3.78 (d, $J_{\text{H-P}} = 13.2$ Hz, 6H); 2.92–2.84 (m, 2H); 1.75 (quint, $J = 7.4$ Hz, 2H); 1.43 (sex, $J = 7.4$ Hz, 2H); 0.93 (t, $J = 7.4$ Hz, 3H). $^{13}\text{C}\{-^1\text{H}\}$ NMR (100 MHz, CDCl_3) δ (ppm) = 53.5 (d, $J_{\text{C-P}} = 5.6$ Hz), 33.2 (d, $J_{\text{C-P}} = 4.6$ Hz), 26.1 (d, $J_{\text{C-P}} = 4.7$ Hz), 22.6, 13.3. ^{31}P NMR (162 MHz, CDCl_3) δ (ppm) = 25.3 (sept, $J_{\text{P-H}} = 13.2$ Hz). ^{77}Se NMR (76 MHz, CDCl_3) δ (ppm) = 95.0 (d, $J_{\text{Se-P}} = 497.2$ and 9.8 Hz). IR (cm^{-1}): 2961, 2844, 1465, 1412, 1210, 989, 812, 723. MS: m/z (rel. int., %) 246 (M^+ , 14.7), 190 (88.4), 109 (100.0), 79 (70.0), 55 (24.8), 41 (23.2). HRMS (APCI-QTOF) calculated mass for $\text{C}_6\text{H}_{15}\text{O}_3\text{PSe} [\text{M}+\text{H}]^+$: 247.0002, found: 246.9998.

4.1.12. *O,O*-dimethyl *Te*-phenyl phosphorotelluroate (3n)

[33] Yield: 0.0553 g (70%); Orange oil. ^1H NMR (400 MHz, CDCl_3) δ (ppm) = 7.84 (dt, $J = 7.7$ and 1.4 Hz, 2H); 7.37 (td, $J = 7.7$ and 1.4 Hz, 1H); 7.26 (t, $J = 7.7$ Hz, 2H); 3.73 (d, $J_{\text{H-P}} = 13.6$ Hz, 6H). $^{13}\text{C}\{-^1\text{H}\}$ NMR (100 MHz, CDCl_3) δ (ppm) = 139.9 (d, $J_{\text{C-P}} = 3.9$ Hz), 129.7 (d, $J_{\text{C-P}} = 1.8$ Hz), 129.0 (d, $J_{\text{C-P}} = 2.2$ Hz), 108.3 (d, $J_{\text{C-P}} = 8.1$ Hz), 53.6 (d, $J_{\text{C-P}} = 5.4$ Hz). ^{31}P NMR (162 MHz, CDCl_3) δ (ppm) = 3.7 (sept, $J_{\text{P-H}} = 13.6$ Hz). $^{125}\text{Te}\{-^1\text{H}\}$ NMR (126 MHz, CDCl_3) δ (ppm) = 349.9 (d, $J_{\text{Te-P}} = 1374.6$ Hz). IR (cm^{-1}): 3011, 2892, 1491, 1483, 1259, 1001, 891, 787. MS: m/z (rel. int., %) 316 (M^+ , 20.7), 207 (12.2), 155 (14.0), 109 (100.0), 79 (20.7), 77 (68.0), 51 (30.3).

4.1.13. *O,O*-diethyl *Te*-phenyl phosphorotelluroate (3°)

[33] Yield: 0.0808 g (94%); Orange oil. ^1H NMR (400 MHz, CDCl_3) δ (ppm) = 7.84 (d, $J = 7.5$ Hz, 2H); 7.36 (t, $J = 7.5$ Hz, 1H); 7.25 (t, $J = 7.5$ Hz, 2H); 4.21–4.06 (m, 4H); 1.31 (t, $J = 7.0$ Hz, 6H). $^{13}\text{C}\{-^1\text{H}\}$ NMR (100 MHz, CDCl_3) δ (ppm) = 139.8 (d, $J_{\text{C-P}} = 3.9$ Hz), 129.6 (d, $J_{\text{C-P}} = 1.6$ Hz), 128.8 (d, $J_{\text{C-P}} = 2.1$ Hz), 108.7 (d, $J_{\text{C-P}} = 8.0$ Hz), 63.4 (d, $J_{\text{C-P}} = 5.5$ Hz), 15.7 (d, $J_{\text{C-P}} = 7.3$ Hz). ^{31}P NMR (162 MHz, CDCl_3) δ (ppm) = -1.1 (quint, $J_{\text{P-H}} = 9.3$ Hz). $^{125}\text{Te}\{-^1\text{H}\}$ NMR (126 MHz, CDCl_3) δ (ppm) = 382.7 (d, $J_{\text{Te-P}} = 1341.8$ Hz). IR (cm^{-1}): 2972, 2861, 1453, 1429, 1220, 983, 880, 717. MS: m/z (rel. int., %) 344 (M^+ , 24.0), 205 (11.5), 137 (18.8), 109 (100.0), 81 (45.1), 77 (65.7), 51 (25.5). HRMS (APCI-QTOF) calculated mass for $\text{C}_{10}\text{H}_{15}\text{O}_3\text{PTe} [\text{M}+\text{H}]^+$: 344.9899, found: 344.9908.

4.1.14. *O,O*-dibutyl *Te*-phenyl phosphorotelluroate (3p)

[32] Yield: 0.0810 g (81%); Orange oil. ^1H NMR (400 MHz, CDCl_3) δ (ppm) = 7.84 (dt, $J = 8.0$ and 1.3 Hz, 2H); 7.36 (td, $J = 7.5$ and

1.3 Hz, 1H); 7.27–7.22 (m, 2H); 4.13–3.99 (m, 4H); 1.63 (quint, $J = 7.4$ Hz, 6H); 1.34 (sex, $J = 7.4$ Hz, 4H); 0.89 (t, $J = 7.4$ Hz, 6H). ^{13}C - $\{^1\text{H}\}$ NMR (100 MHz, CDCl_3) δ (ppm) = 139.9 (d, $J_{\text{C-P}} = 4.1$ Hz), 129.6 (d, $J_{\text{C-P}} = 1.7$ Hz), 128.8 (d, $J_{\text{C-P}} = 2.2$ Hz), 108.8 (d, $J_{\text{C-P}} = 8.1$ Hz), 67.2 (d, $J_{\text{C-P}} = 6.2$ Hz), 31.9 (d, $J_{\text{C-P}} = 7.3$ Hz), 18.7, 13.5. ^{31}P NMR (162 MHz, CDCl_3) δ (ppm) = -0.9 (quint, $J_{\text{P-H}} = 8.1$ Hz) ^{125}Te - $\{^1\text{H}\}$ NMR (126 MHz, CDCl_3) δ (ppm) = 381.4 (d, $J_{\text{Te-P}} = 1337.1$ Hz). IR (cm^{-1}): 2947, 2841, 1478, 1437, 1230, 996, 850, 741. MS: m/z (rel. int., %) 400 (M^+ , 17.8), 342 (6.1), 288 (22.3), 206 (12.5), 137 (60.9), 77 (51.6), 57 (100.0). HRMS (APCI-QTOF) calculated mass for $\text{C}_{14}\text{H}_{23}\text{O}_3\text{P}\text{Te}$ $[\text{M}+\text{H}]^+$: 401.0525, found: 401.0525.

4.1.15. *O,O*-dibenzyl *Te*-phenyl phosphorotelluroate (3q)

[32] Yield: 0.0936 g (80%); Yellow oil. ^1H NMR (400 MHz, CDCl_3) δ (ppm) = 7.75 (d, $J = 7.8$ Hz, 2H); 7.37–7.30 (m, 7H); 7.27–0.724 (m, 4H); 7.18 (t, $J = 7.8$ Hz, 2H); 5.08 (dd, $J = 8.6$ and 3.2 Hz, 4H). ^{13}C - $\{^1\text{H}\}$ NMR (100 MHz, CDCl_3) δ (ppm) = 140.2 (d, $J_{\text{C-P}} = 3.9$ Hz), 135.2 (d, $J_{\text{C-P}} = 7.8$ Hz), 129.6 (d, $J_{\text{C-P}} = 2.0$ Hz), 128.9 (d, $J_{\text{C-P}} = 2.1$ Hz), 128.5, 128.5, 128.1, 108.5 (d, $J_{\text{C-P}} = 8.0$ Hz), 68.7 (d, $J_{\text{C-P}} = 5.8$ Hz). ^{31}P NMR (162 MHz, CDCl_3) δ (ppm) = -1.8 (quint, $J_{\text{P-H}} = 8.6$ Hz). ^{125}Te - $\{^1\text{H}\}$ NMR (126 MHz, CDCl_3) δ (ppm) = 424.7 (d, $J_{\text{Te-P}} = 1387.4$ Hz). IR (cm^{-1}): 3007, 2866, 1476, 1419, 1279, 1021, 895, 756. MS: m/z (rel. int., %) 468 (M^+ , 0.6), 207 (3.0), 91 (100.0), 78 (28.5), 65 (14.4), 51 (20.7). HRMS (APCI-QTOF) calculated mass for $\text{C}_{20}\text{H}_{19}\text{O}_3\text{P}\text{Te}$ $[\text{M}+\text{H}]^+$: 469.0212, found: 469.0208.

4.1.16. *O,O*-dimethyl *Te*-(*p*-tolyl) phosphorotelluroate (3s)

[33] Yield: 0.0742 g (90%); Brown oil. ^1H NMR (400 MHz, CDCl_3) δ (ppm) = 7.72 (d, $J = 7.3$ Hz, 2H); 7.07 (d, $J = 7.3$ Hz, 2H); 3.72 (d, $J_{\text{H-P}} = 13.5$ Hz, 6H); 2.34 (s, 3H). ^{13}C - $\{^1\text{H}\}$ NMR (100 MHz, CDCl_3) δ (ppm) = 140.1 (d, $J_{\text{C-P}} = 3.7$ Hz), 139.3 (d, $J_{\text{C-P}} = 2.7$ Hz), 130.7 (d, $J_{\text{C-P}} = 2.1$ Hz), 104.1 (d, $J_{\text{C-P}} = 8.1$ Hz), 53.5 (d, $J_{\text{C-P}} = 5.3$ Hz), 21.2. ^{31}P NMR (162 MHz, CDCl_3) δ (ppm) = 3.8 (sept, $J_{\text{P-H}} = 13.5$ Hz). ^{125}Te - $\{^1\text{H}\}$ NMR (126 MHz, CDCl_3) δ (ppm) = 346.7 (d, $J_{\text{Te-P}} = 1390.3$ Hz). IR (cm^{-1}): 2957, 2830, 1478, 1461, 1227, 985, 877, 747. MS: m/z (rel. int., %) 330 (M^+ , 23.4), 298 (11.1), 221 (15.3), 169 (17.1), 109 (78.5), 91 (100.0), 79 (16.9), 65 (37.3), 44 (6.34). HRMS (APCI-QTOF) calculated mass for $\text{C}_9\text{H}_{13}\text{O}_3\text{P}\text{Te}$ $[\text{M}+\text{H}]^+$: 330.9743, found: 330.9748.

4.1.17. *Te*-butyl *O,O*-dimethyl phosphorotelluroate (3u)

[32] Yield: 0.0422 g (57%); Orange oil. ^1H NMR (400 MHz, CDCl_3) δ (ppm) = 3.66 (d, $J_{\text{H-P}} = 13.6$ Hz, 6H); 2.81 (dt, $J = 12.8$ Hz and $J = 6.4$, 2H); 1.77 (quint, $J = 7.4$ Hz, 2H); 1.33 (sex, $J = 7.4$ Hz, 2H); 0.86 (d, $J = 7.4$ Hz, 3H). ^{13}C - $\{^1\text{H}\}$ NMR (100 MHz, CDCl_3) δ (ppm) = 53.2 (d, $J_{\text{C-P}} = 5.3$ Hz), 34.3 (d, $J_{\text{C-P}} = 3.5$ Hz), 24.8, 13.2, 8.6 (d, $J_{\text{C-P}} = 3.9$ Hz). ^{31}P NMR (162 MHz, CDCl_3) δ (ppm) = 1.6 (sept, $J_{\text{P-H}} = 13.5$ Hz). ^{125}Te NMR (126 MHz, CDCl_3) δ (ppm) = 91.4 (d, $J_{\text{Te-P/Te-H}} = 1391.7$ and 22.0 Hz). IR (cm^{-1}): 2961, 2839, 1477, 1434, 1263, 1002, 840, 717. MS: m/z (rel. int., %) 296 (M^+ , 14.7), 240 (54.0), 238 (50.8), 109 (100.0), 93 (17.6), 79 (33.1), 57 (31.9), 41 (28.1).

4.2. Biological materials and methods

4.2.1. Animals

The experiments were conducted using male adult Swiss mice (25–35 g) from our own breeding colony. The animals were kept in a separate animal room, on a 12 h light/dark cycle with lights on at 7:00 a.m., at room temperature (22 ± 1 °C) with free access to water and food. The animals were used according to the guidelines of the Committee on Care and Use of Experimental Animal Resources, the Federal University of Pelotas, Brazil (13,008–2020). All efforts were made to minimize animals suffering and to reduce the number of animals used in the experiments.

4.2.2. *In vitro* assays

Phosphorochalcogenoates **3a**, **3c**, **3d**, **3f** and **3g** and positive control, trolox (10 μM), were dissolved in dimethyl sulfoxide (DMSO) for all *in vitro* assays. Mice were euthanized and samples of the whole brain were rapidly removed, placed on ice and weighed. Tissues were immediately homogenized in cold 50 mM Tris–HCl, pH 7.4 (1/5, weight/volume, w/v). The homogenate was centrifuged for 10 min at 2400 g for 10 min at 4 °C to yield a pellet that was discarded, and a low-speed supernatant (S1) was obtained. S1 was used to carry out the effect of compounds **3a**, **3c**, **3d**, **3f** and **3g** on lipid peroxidation and reactive species levels.

4.2.3. Lipid peroxidation assay

Lipid peroxidation in the cerebral tissue was performed by the formation of thiobarbituric acid reactive species (TBARS) during an acid-heating reaction as previously described by Ohkawa, Ohishi and Yagi [72]. The 20 μL aliquot of the brain total was pre-incubated in the presence of compounds (10–500 μM) with sodium nitroprusside (30 mM) at 37 °C for 1 h. The sodium nitroprusside was used as classical inductors of lipid peroxidation. The mixture was then incubated with sodium dodecyl sulfate (SDS, 8.1%), TBA (0.8%), and acetic acid/HCl (pH 3.4) at 95 °C for 2 h. Malondialdehyde (MDA), an end product of the peroxidation of lipids, was used as a biomarker of fatty acid peroxidation. The absorbance of the sample was measured at 532 nm. Results are expressed as percentage of lipid peroxidation.

4.2.4. Reactive species assay

To estimate the level of reactive species production, samples of brain total were incubated with 10 μL of dichlorofluorescein (DCF; 1 mM) in the presence or the absence of a pro-oxidant (sodium azide; 1 mM) and compound (1–500 μM). The reactive species levels were determined by a spectrofluorimetric method, using 2',7'-dichlorofluorescein diacetate (DCHF-DA) assay. The oxidation of DCHF-DA to fluorescent dichlorofluorescein (DCF) is measured for the detection of intracellular reactive species. The DCF fluorescence intensity emission was recorded at 520 nm (with 488 nm excitation) 30 min after the addition of DCHF-DA to the medium [73]. The reactive species levels were expressed as arbitrary units of fluorescence.

4.2.5. Ferric ion reducing antioxidant power

The ferric ion reducing antioxidant power (FRAP) assay evaluate the ability of the compounds to reduce the ferric ions [74]. Different concentrations of compounds (10–500 μM) and FRAP reagent (FeCl_3 , triazine and sodium acetate buffer pH 3.2; 10:1:1) were mixed and the mixture was incubated at 37 °C for 40 min in the dark. The absorbance of the resulting solution was measured at 593 nm.

4.2.6. 2,2-Diphenyl-1-picrylhydrazyl radical scavenging activity

The scavenger activity of the 2,2-diphenyl-1-picrylhydrazyl (DPPH) radical was evaluated according to the methodology of the literature with some modifications [75]. For this assay different concentrations (10–500 μM) of the phosphoroselenoates were mixed with 990 μL of an ethanolic solution containing the DPPH (50 μM) radicals. Subsequently, this mixture was stirred and incubated for 30 min at 30 °C in the dark. Thereafter, the absorbance was read at a wavelength of 517 nm, which the decrease in absorbance indicates the neutralization of the DPPH radicals.

4.2.7. Azinobis-3-ethyl-benzothiazoline-6-sulfonic acid radical scavenging activity

The neutralization evaluation of the radiation of azinobis-3-ethyl-benzothiazoline-6-sulfonic acid (ABTS+) by

phosphoroselenoate was carried out according to a description methodology [76] with some modifications. Different concentrations of compounds (10–500 μM) were mixed with 990 μL the ABTS⁺ solution. The decrease in absorbance was measured at 734 nm, which depicted the scavenging activity of compounds against ABTS radical.

4.2.8. *Ex vivo* assays

Considering that the *in vitro* experiments pointed out the antioxidant properties of compounds, the **3a**, **3c**, **3d**, **3f** and **3g** were used to investigate its *ex vivo* antioxidant effect in the brain, kidney, and liver of Swiss mice.

Mice were divided into 6 groups of 5–6 animals each. Animals belonging to group I received oral application of canola oil (10 mL/kg of body weight). Mice of groups II, III, IV, V and VI received oral administration of **3a**, **3c**, **3d**, **3f** and **3g** (10 mg/kg, intragastric route), respectively. Thirty minutes after the treatment, mice were slightly anesthetized with isoflurane for blood collection by heart puncture in tubes containing heparin. After that the mice were killed and the samples of liver, kidneys and brain were quickly removed. The organs were homogenized as described in Section 4.2.2. The low-speed supernatants (S_1) were separated and used for *ex vivo* assays.

It is important to mention that the dose (10 mg/kg) of the compounds and the time (30 min) were determined based on previous studies by our research group, which tested other organic selenium compounds showed antioxidant effect in male Swiss mice in these same dose and time [77,78].

4.2.9. Lipid peroxidation assay

This assay was carried out with an aliquot of S_1 (20 μL) as described in Section 4.2.3., excepting for the absence of the pre-incubation step.

4.2.10. Superoxide dismutase (SOD) activity

S_1 was diluted 1:10 (v/v) for determination of SOD activity in the test day. Aliquots of supernatant were added in a Na_2CO_3 buffer 50 mM pH 10.3. Enzymatic reaction was started by adding of epinephrine. The color reaction was spectrophotometrically measured at 480 nm. One unit of enzyme was defined as the amount of enzyme required to inhibit the rate of epinephrine autoxidation by 50% at 26 °C [79]. The enzymatic activity was expressed as U/mg protein.

4.2.11. Glutathione peroxidase (GPx) activity

GPx activity in S_1 was assayed spectrophotometrically by the method of Wendel [80], through the GSH/NADPH/glutathione reductase system, by the dismutation of H_2O_2 at 340 nm. S_1 was added in GSH/NADPH/glutathione reductase system and the enzymatic reaction was initiated by adding H_2O_2 . In this assay, the enzyme activity was indirectly measured by means of NADPH decay. H_2O_2 is reduced and generates GSSG from GSH. GSSG is regenerated back to GSH by glutathione reductase present in the assay media at the expenses of NADPH. The enzymatic activity was expressed as nmol NADPH/min/mg protein.

4.2.12. Toxicological parameters

In order to investigate the effects of compounds on toxicological parameters, plasma was obtained by centrifugation at 200 \times g for 10 min (hemolyzed plasma was discarded) and the activities of ALT and AST, and the levels of urea and creatinine were determined using commercial kits (Labtest, Diagnostica S.A., Minas Gerais, Brazil).

4.2.13. Statistical analysis

The results as means \pm standard error of the mean (SEM) for the experiments data were performed using one-way analysis of variance followed by Tukey test when appropriated and *Student-t* test. All tests were performed at least three times in duplicate. The *p* values less than 0.05 ($p < 0.05$) were considered as indicative of significance.

Declaration of competing interest

The authors declare that they have no known competing financial interests or personal relationships that could have appeared to influence the work reported in this paper.

Acknowledgements

This study was financed in part by the Coordenação de Aperfeiçoamento de Pessoal de Nível Superior - Brasil (CAPES) - Finance Code 001. FAPERGS (PqG 17/2551-0000987-8) and FAPERGS/CAPES April 2018 - DOCFIX 18/2551-0000511-8, CNPq and FINEP are acknowledged for financial support.

Appendix A. Supplementary data

Supplementary data to this article can be found online at <https://doi.org/10.1016/j.ejmech.2020.113052>.

References

- [1] Z. Chen, D. Luo, X. Luo, M. Kang, Z. Lin, Two-dimensional assembly of tetrahedral chalcogenide clusters with tetrakis(imidazolyl)borate ligands, *Dalton Trans.* 41 (2012) 3942–3944, <https://doi.org/10.1039/C2DT12043G>.
- [2] R. Stieler, F. Bublitz, R.A. Burrow, G.N.M. de Oliveira, M.A. Villetti, M.B. Pereira, P. Piquini, E.S. Lang, Synthesis and characterization of $[\text{Cd}_8\text{Cl}_2\text{Se}(\text{SePh})_{12}(\text{PCy}_3)_2] \cdot 2.5\text{CH}_3\text{OH}$, *J. Braz. Chem. Soc.* 21 (2010) 2146–2154, <https://doi.org/10.1590/S0103-50532010001100017>.
- [3] E.P. Wendler, A.A. dos Santos, The use of butyl organotellurides in the synthesis of natural bioactive compounds, *Synlett* (2009) 1034–1040, <https://doi.org/10.1055/s-0028-1088219>.
- [4] I.P. Beletskaya, V.P. Ananikov, Transition-metal-catalyzed C–S, C–Se, and C–Te bond formation via cross-coupling and atom-economic addition reactions, *Chem. Rev.* 111 (2011) 1596–1636, <https://doi.org/10.1021/cr100347k>.
- [5] D. Alves, B. Goldani, E.J. Lenardão, G. Perin, R.F. Schumacher, M.W. Paixão, Copper catalysis and organocatalysis showing the way: synthesis of selenium-containing highly functionalized 1,2,3-triazoles, *Chem. Rec.* 18 (2018) 527–542, <https://doi.org/10.1002/tcr.201700058>.
- [6] M.C.D.F. Xavier, B. Goldani, R.F. Schumacher, G. Perin, P.H. Schneider, D. Alves, Silver-catalyzed direct selenylation of terminal alkynes through C–H bond functionalization, *Mol. Catal.* 427 (2017) 73–79, <https://doi.org/10.1016/j.molcata.2016.11.033>.
- [7] A.M.S. Recchi, D.F. Back, G. Zeni, Sequential carbon–carbon/carbon–selenium bond formation mediated by iron(III) chloride and diorganyl diselenides: synthesis and reactivity of 2-organoselenyl-naphthalenes, *J. Org. Chem.* 82 (2017) 2713–2723, <https://doi.org/10.1021/acs.joc.7b00050>.
- [8] G. Perin, E.J. Lenardão, R.G. Jacob, R.B. Panatieri, Synthesis of vinyl selenides, *Chem. Rev.* 109 (2009) 1277–1301, <https://doi.org/10.1021/cr8004394>.
- [9] N. Petragnani, H.A. Stefani, *Tellurium in Organic Synthesis*, Elsevier Ltd, Oxford, UK, 2007.
- [10] D. Alves, C.G. Santos, M.W. Paixão, L.C. Soares, D. de Souza, O.E.D. Rodrigues, A.L. Braga, CuO nanoparticles: an efficient and recyclable catalyst for cross-coupling reactions of organic diselenides with aryl boronic acids, *Tetrahedron Lett.* 50 (2009) 6635–6638, <https://doi.org/10.1016/j.tetlet.2009.09.052>.
- [11] A. Kumar, S. Kumar, A convenient and efficient copper-catalyzed synthesis of unsymmetrical and symmetrical diaryl chalcogenides from arylboronic acids in ethanol at room temperature, *Tetrahedron* 70 (2014) 1763–1772, <https://doi.org/10.1016/j.tet.2014.01.030>.
- [12] M.Z. Kassae, E. Motamedi, B. Movassagh, S. Poursadeghi, Iron-catalyzed formation of C–Se and C–Te bonds through cross coupling of aryl halides with Se(0) and Te(0)/Nano-Fe₃O₄@GO, *Synthesis* 45 (2013) 2337–2342, <https://doi.org/10.1055/s-0033-1338488>.
- [13] M. Soleiman-Beigi, M. Hemmati, An efficient, one-pot and CuCl-catalyzed route to the synthesis of symmetric organic disulfides via domino reactions of thioacetamide and aryl (alkyl) halides, *Appl. Organomet. Chem.* 27 (2013) 734–736, <https://doi.org/10.1002/aoc.3074>.
- [14] C. Santi, R.G. Jacob, B. Monti, L. Bagnoli, L. Sancineto, E.J. Lenardão, Water and aqueous mixtures as convenient alternative media for organoselenium

- chemistry, *Molecules* 21 (2016) 1482–1499, <https://doi.org/10.3390/molecules21111482>.
- [15] C. Santi, Perspective in green chemistry for organoselenium compounds (no more an oxymoron), *Curr. Green Chem.* 6 (2019) 9–11, <https://doi.org/10.2174/221334610601190329164654>.
- [16] C. Lopin, G. Gouhier, A. Gautier, S.R. Piettre, Phosphonyl, phosphonothioyl, phosphonodithioyl, and phosphonotrithioyl radicals: generation and study of their addition onto alkenes, *J. Org. Chem.* 68 (2003) 9916–9923, <https://doi.org/10.1021/jo0348064>.
- [17] L.-B. Han, N. Choi, M. Tanaka, Facile oxidative addition of the phosphorus–selenium bond to Pd(0) and Pt(0) complexes and development of Pd-catalyzed regio- and stereoselective selenophosphorylation of alkynes, *J. Am. Chem. Soc.* 118 (1996) 7000–7001, <https://doi.org/10.1021/ja9608860>.
- [18] N.M. Yousif, K.Z. Gadalla, S.M. Yassin, Synthesis of *O,O*-dialkyl *S*-phenyl phosphorothiolates- and dithiolates, phosphorus, sulfur, silicon relay, *Elements* 60 (1991) 261–263, <https://doi.org/10.1080/10426509108036789>.
- [19] M. Fukuoka, S. Shuto, N. Minakawa, Y. Ueno, A. Matsuda, Alternative synthesis of cyclic IDP-carbocyclic ribose. Efficient cyclization of an 8-bromo-*N*¹-[5-(phosphoryl)carbocyclic-ribosyl]inosine 5'-phenylthiophosphate derivative mediated by iodine, *Tetrahedron Lett.* 40 (1999) 5361–5364, [https://doi.org/10.1016/S0040-4039\(99\)00977-6](https://doi.org/10.1016/S0040-4039(99)00977-6).
- [20] M. Marinuzzi, M.C. Fulco, R. Rizzo, R. Pellicciari, Synthesis of novel unsymmetrically bridgehead-substituted phenylseleno bicyclo[1.1.1]pentanes, *Synlett* (2004) 1027–1028, <https://doi.org/10.1055/s-2004-822882>.
- [21] A. Gautier, G. Garipova, E. Dubert, H. Oulyadi, S.R. Piettre, Efficient and practical aerobic radical addition of thiophosphites to alkenes, *Tetrahedron Lett.* 42 (2001) 5673–5676, [https://doi.org/10.1016/S0040-4039\(01\)01074-7](https://doi.org/10.1016/S0040-4039(01)01074-7).
- [22] P. Das, J.T. Njardarson, Anionic cascade routes to sulfur and nitrogen heterocycles originating from thio- and aminophosphate precursors, *Eur. J. Org. Chem.* (2016) 4249–4259, <https://doi.org/10.1002/ejoc.201600312>.
- [23] E.A. Ilardi, E. Vitaku, J.T. Njardarson, Data-mining for sulfur and fluorine: an evaluation of pharmaceuticals to reveal opportunities for drug design and discovery, *J. Med. Chem.* 57 (2014) 2832–2842, <https://doi.org/10.1021/jm401375q>.
- [24] T.S. Kumar, T. Yang, S. Mishra, C. Cronin, S. Chakraborty, J.-B. Shen, B.T. Liang, K.A. Jacobson, 5'-Phosphate and 5'-phosphonate ester derivatives of (*N*)-methanocarba adenosine with *in vivo* cardioprotective activity, *J. Med. Chem.* 56 (2013) 902–914, <https://doi.org/10.1021/jm301372c>.
- [25] A. Hughes, *Amino Acids, Peptides, and Proteins in Organic Chemistry: Modified Amino Acids, Organocatalysis and Enzyme*, Wiley-VCH, Weinheim, Germany, 2009.
- [26] F.H. Westheimer, Why nature chose phosphates, *Science* 235 (1987) 1173–1178, <https://doi.org/10.1126/science.2434996>.
- [27] F.R. Hartley, The chemistry of organophosphorus compounds: ter- and quinque-valent phosphorus acids and their derivatives, in: S. Patai (Ed.), *Patai's Chemistry of Functional Groups*, John Wiley & Sons, Chichester, England, 1996.
- [28] J. Golebiewska, M. Rachwalak, T. Jakubowski, J. Romanowska, J. Stawinski, Reaction of boranephosphonate diesters with amines in the presence of iodine: the case for the intermediacy of *H*-phosphonate derivatives, *J. Org. Chem.* 83 (2018) 5496–5505, <https://doi.org/10.1021/acs.joc.8b00419>.
- [29] G. Mugesh, W.-W. du Mont, H. Sies, Chemistry of biologically important synthetic organoselenium compounds, *Chem. Rev.* 101 (2001) 2125–2180, <https://doi.org/10.1021/cr000426w>.
- [30] E.J. Lenardão, C. Santi, L. Sancineto, *New Frontiers in Organoselenium Compounds*, Springer, Basel, Switzerland, 2018.
- [31] C.W. Nogueira, G. Zeni, J.B.T. Rocha, Organoselenium and organotellurium compounds: toxicology and pharmacology, *Chem. Rev.* 104 (2004) 6255–6286, <https://doi.org/10.1021/cr0406559>.
- [32] J.-M. Chen, X. Huang, A facile preparation of organytellurophosphates, *Synth. Commun.* 34 (2004) 1745–1752, <https://doi.org/10.1081/SCC-120030762>.
- [33] Q. Xu, C.-G. Liang, X. Huang, Free radical reaction of dialkyl phosphites and organophosphonates: a new facile and convenient preparation of arylselenophosphates, *Synth. Commun.* 33 (2003) 2777–2785, <https://doi.org/10.1081/SCC-120022165>.
- [34] N. Petragiani, V.G. Toscano, M.M. Campos, Selenophosphororganische Verbindungen, II, *Chem. Ber.* 101 (1968) 3070–3078, <https://doi.org/10.1002/cher.19681010916>.
- [35] Y.-X. Gao, G. Tang, Y. Cao, Y.-F. Zhao, A Novel and General Method for the Formation of *S*-Aryl, *Se*-Aryl, and *Te*-Aryl Phosphorochalcogenates, 2009, pp. 1081–1086, <https://doi.org/10.1055/s-0028-1088012>. Synthesis.
- [36] S. Mitra, S. Mukherjee, S.K. Sen, A. Harja, Environmentally benign synthesis and antimicrobial study of novel chalcogenophosphates, *Bioorg. Med. Chem. Lett.* 24 (2014) 2198–2201, <https://doi.org/10.1016/j.bmcl.2014.03.008>.
- [37] S. Chen, J. Chen, X. Xu, Y. He, R. Yi, R. Qiu, Calix[4]arene-assisted KOH-catalyzed synthesis of *O,O*-dialkyl-*Se*-aryl phosphoroselenoates, *J. Organomet. Chem.* 818 (2016) 123–127, <https://doi.org/10.1016/j.jorganchem.2016.06.010>.
- [38] S.K. Bhunia, P. Das, R. Jana, Atom-economical selenation of electron-rich arenes and phosphonates with molecular oxygen at room temperature, *Org. Biomol. Chem.* 16 (2018) 9243–9250, <https://doi.org/10.1039/C8OB02792G>.
- [39] M. Mondal, A. Saha, Benign synthesis of thiophosphates, thiophosphinates and selenophosphates in neat condition using *N*-chalcogenoimides as the source of electrophilic sulfur/selenium, *Tetrahedron Lett.* 60 (2019) 150965, <https://doi.org/10.1016/j.tetlet.2019.150965>.
- [40] X. Zhang, Z. Shi, C. Shao, J. Zhao, D. Wang, D. Zhang, L. Li, Three-component coupling reaction in water: a one-pot protocol for the construction of P–S–C(sp³) and P–Se–C(sp³) bonds, *Eur. J. Org. Chem.* (2017) 1884–1888, <https://doi.org/10.1002/ejoc.201700344>.
- [41] Y. Moon, Y. Moon, H. Choi, S. Hong, Metal- and oxidant-free S–P(O) bond construction via direct coupling of P(O)H with sulfinic acids, *Green Chem.* 19 (2017) 1005–1013, <https://doi.org/10.1039/C6GC03285K>.
- [42] J. Bai, X. Cui, H. Wang, Y. Wu, Copper-catalyzed reductive coupling of aryl sulfonyl chlorides with *H*-phosphonates leading to *S*-aryl phosphorothioates, *Chem. Commun.* 50 (2014) 8860–8863, <https://doi.org/10.1039/C4CC02693D>.
- [43] T. Lönnberg, Sulfurization of *H*-phosphonate diesters by elemental sulfur under aqueous conditions, *ACS Omega* 2 (2017) 5122–5127, <https://doi.org/10.1021/acsomega.7b00970>.
- [44] R.D. Crocker, M.A. Hussein, J. Ho, T.V. Nguyen, NHC-Catalyzed metathesis and phosphorylation reactions of disulfides: development and mechanistic insights, *Chem. Eur. J.* 23 (2017) 6259–6263, <https://doi.org/10.1002/chem.201700744>.
- [45] M. Xia, J. Cheng, Catalyst- and oxidant-free coupling of disulfides with *H*-phosphine oxide: construction of P–S bond leading to thiophosphinates, *Tetrahedron Lett.* 57 (2016) 4702–4704, <https://doi.org/10.1016/j.tetlet.2016.09.021>.
- [46] J.-W. Xue, M. Zeng, S. Zhang, Z. Chen, G. Yin, Lewis acid promoted aerobic oxidative coupling of thiols with phosphonates by simple nickel(II) catalyst: substrate scope and mechanistic studies, *J. Org. Chem.* 84 (2019) 4179–4190, <https://doi.org/10.1021/acs.joc.9b00194>.
- [47] G. Kumaraswamy, R. Raju, Copper(I)-induced sulfenylation of *h*-phosphonates, *H*-phosphonites and phosphine oxides with aryl/alkylsulfonylhydrazides as a thiol surrogate, *Adv. Synth. Catal.* 356 (2014) 2591–2598, <https://doi.org/10.1002/adsc.201400116>.
- [48] F. Chen, G. Huang, Antioxidant activity of polysaccharides from different sources of ginseng, *Int. J. Biol. Macromol.* 125 (2019) 906–908, <https://doi.org/10.1016/j.ijbiomac.2018.12.134>.
- [49] J. Chen, G. Huang, Antioxidant activities of garlic polysaccharides and its phosphorylated derivative, *Int. J. Biol. Macromol.* 125 (2019) 432–435, <https://doi.org/10.1016/j.ijbiomac.2018.12.073>.
- [50] F. Chen, G. Huang, Z. Yang, Y. Hou, Antioxidant activity of Momordica charantia polysaccharide and its derivatives, *Int. J. Biol. Macromol.* 138 (2019) 673–680, <https://doi.org/10.1016/j.ijbiomac.2019.07.129>.
- [51] L. Chen, G. Huang, Antioxidant activities of phosphorylated pumpkin polysaccharide, *Int. J. Biol. Macromol.* 125 (2019) 256–261, <https://doi.org/10.1016/j.ijbiomac.2018.12.069>.
- [52] Y. Liu, G. Huang, The antioxidant activities of carboxymethylated cushaw polysaccharide, *Int. J. Biol. Macromol.* 121 (2019) 666–670, <https://doi.org/10.1016/j.ijbiomac.2018.10.108>.
- [53] X. Xiong, G. Huang, H. Huang, The antioxidant activities of phosphorylated polysaccharide from native ginseng, *Int. J. Biol. Macromol.* 126 (2019) 842–845, <https://doi.org/10.1016/j.ijbiomac.2018.12.266>.
- [54] B.G. Janesko, H.C. Fisher, M.J. Bridle, J.-L. Montchamp, P(=O, H) to P–OH tautomerism: a theoretical and experimental study, *J. Org. Chem.* 80 (2015) 10025–10032, <https://doi.org/10.1021/acs.joc.5b01618>.
- [55] M. Sobkowski, A. Kraszewski, J. Stawinski, Recent advances in *H*-phosphonate chemistry. part 2. synthesis of C-phosphonate derivatives, *Top. Curr. Chem.* 361 (2015) 179–216, https://doi.org/10.1007/128_2014_563.
- [56] X. Chen, Z. Xiao, H. Chu, B. Wang, A.-Y. Peng, Reinvestigation of the iodine-mediated phosphoramidation reaction of amines and P(OR)₃ and its synthetic applications, *Org. Biomol. Chem.* 16 (2018) 6783–6790, <https://doi.org/10.1039/C8OB01840E>.
- [57] J.E. Nycz, G. Malecki, S. Chikkali, I. Hajdok, P. Singh, Reaction of quinoline-5,8-diones with selected charged phosphorus nucleophiles, Phosphorus, Sulfur, and Silicon 187 (2012) 564–572, <https://doi.org/10.1080/10426507.2011.626472>.
- [58] J.D. Woollins, R.S. Laitinen (Eds.), *Selenium and Tellurium Chemistry, Chapter 2: New Selenium Electrophiles and Their Reactivity*, Springer-Verlag Berlin, Heidelberg, 2011.
- [59] D.R. Joshi, N. Adhikari, An overview on common organic solvents and their toxicity, *J. Pharm. Res. Int.* 28 (2019) 1–18, <https://doi.org/10.9734/JPR/2019/v28i330203>.
- [60] B. Halliwell, Reactive oxygen species and the central nervous system, *J. Neurochem.* 59 (1992) 1609–1623, <https://doi.org/10.1111/j.1471-4159.1992.tb10990.x>.
- [61] J.B. Rodriguez, C. Gallo-Rodriguez, The role of the phosphorus atom in drug design, *ChemMedChem* 14 (2019) 190–216, <https://doi.org/10.1002/cmdc.201800693>.
- [62] H. Liu, Z. Shi, J. Li, P. Zhao, S. Qin, Z. Nie, The impact of phosphorus supply on selenium uptake during hydroponics experiment of winter wheat (*Triticum aestivum*) in China, *Front. Plant Sci.* 9 (2018) 373, <https://doi.org/10.3389/fpls.2018.00373>.
- [63] E. Zoidis, I. Seremelis, N. Kontopoulos, G.P. Danezis, Selenium-dependent antioxidant enzymes: actions and properties of selenoproteins, *Antioxidants* 7 (2018) 66–92, <https://doi.org/10.3390/antiox7050066>.
- [64] W. Droge, Free radicals in the physiological control of cell function, *Physiol. Rev.* 82 (2002) 47–95, <https://doi.org/10.1152/physrev.00018.2001>.
- [65] K. Facecchia, L.A. Fochesato, S.D. Ray, S.J. Stohs, S. Pandey, Oxidative toxicity in neurodegenerative diseases: role of mitochondrial dysfunction and therapeutic strategies, *J. Toxicol.* 683728 (2011), <https://doi.org/10.1155/2011/683728>.

- [66] B. Halliwell, *Biochemistry of Oxidative Stress*, Portland Press Limited, 2007.
- [67] T.M. Michel, D. Pulschen, J. Thome, The role of oxidative stress in depressive disorders, *Curr. Pharmaceut. Des.* 18 (2012) 5890–5899, <https://doi.org/10.2174/138161212803523554>.
- [68] E. Cadenas, K.J. Davies, Mitochondrial free radical generation, oxidative stress, and aging, *Free Radic. Biol. Med.* 29 (2000) 222–230, [https://doi.org/10.1016/S0891-5849\(00\)00317-8](https://doi.org/10.1016/S0891-5849(00)00317-8).
- [69] I. Tumosiėnė, K. Kantminienė, A. Klevinskas, V. Petrikaitė, I. Jonuskienė, V. Mickevičius, Antioxidant and anticancer activity of novel derivatives of 3-[(4-methoxyphenyl)amino]propanehydrazide, *Molecules* 25 (2020), <https://doi.org/10.3390/molecules25132980>, 2980–2300.
- [70] D. Puthran, B. Poojar, N. Purushotham, N. Harikrishna, S.G. Nayaka, V. Kamata, Synthesis of novel Schiff bases using 2-Amino-5-(3-fluoro-4-methoxyphenyl) thiophene-3-carbonitrile and 1,3-Disubstituted pyrazole-4-carboxaldehydes derivatives and their antimicrobial activity, *Heliyon* 5 (2019), <https://doi.org/10.1016/j.heliyon.2019.e02233> e02233–e02239.
- [71] H. Huang, W. Wang, X. Xu, C. Zhu, Y. Wang, J. Liu, W. Lia, W. Fu, Discovery of 3-((dimethylamino)methyl)-4-hydroxy-4-(3-methoxyphenyl)-N-phenyl-piperidine-1 carboxamide as novel potent analgesic, *Eur. J. Med. Chem.* 189 (2020) 112070–112084, <https://doi.org/10.1016/j.ejmech.2020.112070>.
- [72] H. Ohkawa, N. Ohishi, K. Yagi, Assay for lipid peroxides in animal tissues by thiobarbituric acid reaction, *Anal. Biochem.* 95 (1979) 351–358, [https://doi.org/10.1016/0003-2697\(79\)90738-3](https://doi.org/10.1016/0003-2697(79)90738-3).
- [73] C. Loetchutinat, S. Kothan, S. Dechsupa, J. Meesungnoen, J.-P. Jay-Gerin, S. Mankhetkorn, Spectrofluorometric determination of intracellular levels of reactive oxygen species in drug-sensitive and drug-resistant cancer cells using the 2', 7'-dichlorofluorescein diacetate assay, *Radiat. Phys. Chem.* 72 (2005) 323–330, <https://doi.org/10.1016/j.radphyschem.2004.09.027>.
- [74] C.W. Choi, S.C. Kim, S.S. Hwang, B.K. Choi, H.J. Ahn, M.Y. Lee, S.H. Park, S.K. Kim, Antioxidant activity and free radical scavenging capacity between Korean medicinal plants and flavonoids by assay-guided comparison, *Plant Sci.* 163 (2002) 1161–1168, [https://doi.org/10.1016/S0168-9452\(02\)00332-1](https://doi.org/10.1016/S0168-9452(02)00332-1).
- [75] W. Brand-Williams, M.-E. Cuvelier, C. Berset, Use of a free radical method to evaluate antioxidant activity, *LWT - Food Sci. Technol. (Lebensmittel-Wissenschaft -Technol.)* 28 (1995) 25–30, [https://doi.org/10.1016/S0023-6438\(95\)80008-5](https://doi.org/10.1016/S0023-6438(95)80008-5).
- [76] R. Re, N. Pellegrini, A. Proteggente, A. Pannala, M. Yang, C. Rice-Evans, Antioxidant activity applying an improved ABTS radical cation decolorization assay, *Free Radic. Biol. Med.* 26 (1999) 1231–1237, [https://doi.org/10.1016/S0891-5849\(98\)00315-3](https://doi.org/10.1016/S0891-5849(98)00315-3).
- [77] P.T. Birmann, A.M. Casaril, D. Hartwig, R.G. Jacob, F.K. Seixas, T. Collares, L. Savegnago, A novel pyrazole-containing selenium compound modulates the oxidative and nitric pathways to reverse the depression-pain syndrome in mice, *Brain Res.* 1741 (2020) 146880–146893, <https://doi.org/10.1016/j.brainres.2020.146880>.
- [78] P.T. Birmann, M. Domingues, A.M. Casaril, T.A. Smaniotto, D. Hartwig, R.G. Jacob, L. Savegnago, A pyrazole-containing selenium compound modulates neuroendocrine, oxidative stress, and behavioral responses to acute restraint stress in mice, *Behav. Brain Res.* 396 (2021), <https://doi.org/10.1016/j.bbr.2020.112874>, 112874–112780.
- [79] H.P. Misra, I. Fridovich, The role of superoxide anion in the autoxidation of epinephrine and a simple assay for superoxide dismutase, *J. Biol. Chem.* 247 (1972) 3170–3175.
- [80] A. Wendel, Glutathione peroxidase, *Methods Enzymol.* 77 (1981) 325–333, [https://doi.org/10.1016/S0076-6879\(81\)77046-0](https://doi.org/10.1016/S0076-6879(81)77046-0).